Protoplasma
https://doi.org/10.1007/s00709-021-01617-1

ORIGINAL ARTICLE

Effects of ethylenediurea (EDU) on apoplast and chloroplast proteome in two wheat varieties under high ambient ozone: an approach to investigate EDU's mode of action

Sunil K. Gupta[1,2,3] · Marisha Sharma[1] · Vivek K. Maurya[1] · Farah Deeba[1,4] · Vivek Pandey[1,2]

Received: 14 July 2020 / Accepted: 22 January 2021

Abstract

Rising tropospheric ozone (O_3) is a serious threat to plants and animals in the present climate change scenario. High tropospheric O_3 has the capability to disrupt cellular organelles leading to impaired photosynthesis and significant yield reduction. Apoplast and chloroplast are two important cellular components in a plant system. Their proteomic response with ethylenediurea (EDU) treatment under tropospheric O_3 has not been explored till date. EDU (an organic compound) protects plants exclusively against harmful O_3 effects through activation of antioxidant defense mechanism. The present study investigated the mode of action of EDU (hereafter MAE) by identifying proteins involved in apoplast and chloroplast pathways. Two wheat varieties viz. Kundan and PBW 343 (hereafter K and P respectively) and three EDU treatments (0= control, 200, and 300 ppm) have been used for the study. In apoplast isolates, proteins such as superoxide dismutase (SOD), amino methyltransferase, catalase, and Germin-like protein have shown active role by maintaining antioxidant defense system under EDU treatment. Differential expression of these proteins leads to enhanced antioxidative defense mechanisms inside and outside the cell. Chloroplast proteins such as Rubisco, Ferredoxin NADP- reductase (FNR), fructose,1-6 bis phosphatase (FBPase), ATP synthase, vacuolar proton ATPase, and chaperonin have regulated their abundance to minimize ozone stress under EDU treatment. After analyzing apoplast and chloroplast protein abundance, we have drawn a schematic representation of the MAE working mechanism. The present study showed that plants can be capable of O_3 tolerance, which could be improved by optimizing the apoplast ROS pool under EDU treatment.

Keywords Apoplast · Chloroplast · EDU protection · Wheat · Ambient ozone · Proteomics · Mass spectrometry

Introduction

In many countries of the world, tropospheric ozone (O_3) pollution has become a significant fundamental threat, causing its adverse effects on crops and the ecosystem (LRTAP 2017; Lefohn et al. 2018; The Royal Society 2008; Fuhrer et al. 2016). Ozone is formed in the troposphere (the lowest part of the earth's atmosphere) when nitrogen oxide and volatile organic compounds in the air interact with photons and break down in a process called photolysis (Wilkinson et al. 2012). The presence of high concentrations of ozone pose a significant threat to various plants and other organisms, as it can cause oxidative damage when it reacts with molecules in living tissues (Long and Naidu 2002; Fiscus et al. 2005; Betzelberger et al. 2012; Wilkinson et al. 2012; Emberson et al. 2018; Chen et al. 2020). The abiotic stress, i.e., ozone, induces the formation of ROS, for instance, hydroxyl radical (HO·), superoxide anion (O_2^- .), and singlet oxygen ($^1O_2$) (Gill and Tuteja 2010; You and Chan 2015). ROS is harmful to organisms in high concentrations, and when these O_2 species exceed its normal range, the cells undergo oxidative stress (Rai 2020). This process involves lipid peroxidation, protein oxidation, damage of nucleic acid, and enzymatic inhibition.

Handling Editor: Bhumi Nath Tripathi

✉ Vivek Pandey
v.pandey@nbri.res.in

[1] Plant Ecology and Climate Change Science Division, CSIR-National Botanical Research Institute, Rana Pratap Marg, Lucknow 226 001, India

[2] Academy of Scientific and Innovative Research (AcSIR), Ghaziabad, Uttar Pradesh 201 002, India

[3] CAS Key Laboratory of Tropical Forest Ecology, Xishuangbanna Tropical Botanical Garden, Chinese Academy of Sciences, Mengla 666 303, Yunnan, China

[4] Biotechnology Department, CSIR-Central Institute of Medicinal and Aromatic Plants, Lucknow 226 015, India

Published online: 28 February 2021

However, under normal conditions, about 1% of O_2 consumed by plants is diverted to produce ROS in various subcellular loci such as chloroplasts, mitochondria, and peroxisomes (Asada 1987; Rai 2020). In addition, to signal perception and transduction, apoplast proteins also contribute to cell wall modification and reconstruction, and defense responses. However, they comprise only 5–10% of the cell wall dry weight (Vandenabeele et al. 2003).

Ozone is taken up into the leaf interior via the stomata (Kerstiens and Lendzian 1989), where it is believed to react with constituents of the aqueous matrix associated with the cell wall (i.e., the apoplast) to yield a suite of reactive oxygen species (ROS) resulting in the oxidation of sensitive components of the plasma-lemma, and subsequently the cytosol (Heath 1980; Chameides 1989). It has been reported that apoplast isolates respond to many abiotic stresses such as air pollutants, heavy metals, drought, salinity, and temperature extremes (Dietz 1997; Schraudner et al. 1992; Fecht-Christoffers et al. 2003; Brune et al. 1994; Covarrubias et al. 1995; Griffith et al. 1992). In the apoplast, ROS detoxification takes place as the ozone enters inside; it can be considered as an apoplastic defense mechanism from the ozone (Kangasjärvi et al. 2005; Castagna and Ranieri 2009). Ascorbate plays a crucial role during the detoxification of ROS and acts as a major redox buffer in the apoplast (Foyer and Noctor 2009). The changes in protein expression (antioxidant enzyme activities) can occur very fast in response to abiotic stress. However, apoplast can produce and maintain an optimum ROS pool in response to various abiotic stresses (Vainonen and Kangasjärvi 2015). Ueda et al. (2015) reported a novel apoplast gene OsORAP1-like ascorbate oxidase overexpressed under ozone stress leading to premature cell death in rice. Overexpression of ascorbate oxidase also impacted ascorbate and glutathione redox state in apoplast during ozone sensitivity (Sanmartin et al. 2003).

Chloroplast originated from an endosymbiotic event, in which an ancestral photosynthetic cyanobacterium was taken up by a heterotrophic host cell that already contained mitochondria (Cavalier-Smith 2000). Some previous studies indicate that one of the main targets of direct pollutant activity is the photosynthetic apparatus (Gupta et al. 2018, 2020). Chen et al. (2020) reported 35% of chloroplast proteins were differentially expressed under ozone stress. Chlorophyll proteins are multi-cofactor protein that binds pigments such as Chl *a*, Chl *b*, and carotenoids (Green and Durnford 1996). Chloroplast proteins, e.g., Rubisco large subunit (LSU) and a small subunit (SSU) showed differential expression under EDU treatments in wheat (Gupta et al. 2018) and maize (Gupta et al. 2020). Some other chloroplast proteins have similar or opposite abundance, but their goal is to maintain better homeostasis during abiotic stress. The structural proteins, for instance, photosystem *b* R (PsbR), photosystem *a* K (PsaK), and photosystem *a* A (PsaA) of PSII and PSI were decreased in their abundance under ozone stress resulting in impaired photosynthetic rate (Roose et al. 2007). Blanco-Ward et al. (2020) reported chlorosis of grapevine leaf under tropospheric ozone pollution. The high tropospheric ozone can distort the ultrastructure of the chloroplast, for instance, conifer-needle (Kivimaenpaa et al. 2005), and reduces their numbers, for instance, grapevine (Chen et al. 2020). The PS II and PS I are two important reaction centers in light reaction. Their working mechanism is also influenced by the high ozone (Tran et al. 2013; Salvatori et al. 2013; Chen et al. 2020). Ozone assessment studies can be carried out through evaluating CO_2 assimilation rate, Rubisco activities/regeneration, and estimating chlorophyll content (Rinnan and Holopainen 2004). Salvatori (2013) showed a decrease in the density of the reaction center per cross-section or leaf area (RC/CS0) and an increase in energy dissipation per reaction center (DI0/RC), and indicated that ozone stress enhanced energy dissipation.

A chemical, N-(2-(2-oxo-1-imidazolidinyl) ethyl)-N'-phenylurea or ethylene diurea (EDU) has been shown to act as an antiozonant with protective effects against ozone injury in plants (Carnahan et al. 1978). The roles of EDU to induce changes in plant homeostasis against ozone stress are well documented (Manning et al. 2011). However, the exact mechanism behind these changes still has a knowledge gap. Many workers tried to investigate the mode of action of EDU (MAE), but it remains to be resolved (Whitaker et al. 1990; Pitcher et al. 1992; Lee et al. 1997; Paoletti et al. 2009). Lee et al. (1997) reported that EDU does not have the antioxidative capability but maintains antioxidants machinery during O_3 stress in cells. EDU may initiate cytokinin production or have cytokinin-like characteristics in protecting chlorophyll from breakdown, increasing protein and RNA synthesis, and stimulating cell growth (Lee and Chen 1982; Whitaker et al. 1990).

In the present study, we initiated a proteomic investigation of MAE by identifying EDU-responsive proteins in the wheat leaf apoplast and chloroplast. This is the first proteomic study of the apoplast and chloroplast isolates in response to EDU, and the results greatly expand our knowledge for drawing a probable MAE and mediated signaling through apoplast in the cell. We have used one dimensional/sodium dodecyl sulfate-polyacrylamide gel electrophoresis (SDS-PAGE) and two-dimensional polyacrylamide gel electrophoresis (2D-PAGE) technique in the present investigation. EDU-mediated changes were observed in apoplast proteins, which were found to be related to defense and antioxidant responses. Effects of EDU were also observed on chloroplast proteins as several related proteins were identified. The abundance changes in these identified proteins, and their putative functions, are consistent with the proposed role of the apoplast and chloroplast under ozone stress, including those of transduction and defense-responsive proteins. The present study will also provide a

framework for analyzing the complexity of apoplast and chloroplast proteins in winter wheat by further functionally characterizing the individual proteins.

Material and methods

Experimental site and meteorological condition

The field experiments were conducted at CSIR-National Botanical Research Institute garden in Lucknow city, (26° 55′ N latitude, 80° 59′ E longitude and at an altitude of 113m), Uttar Pradesh, India. Twenty-four plots of $9m^2$ were prepared. Plots were randomized using a random number generator to sow seeds and treatments with the statistical software tool (SPSS Inc., version 16). A dry, tropical monsoon climate characterizes Lucknow. The maximum temperature recorded during the experimental period was in March (29°C), whereas the minimum temperature was in January (13°C). A minimum of 51% and a maximum of 84% humidity were recorded during the study period.

Biological material

Wheat (*Triticum aestivum* L.) variety Kundan (released in 2001) and PBW 343 (released in 1996) selected for the experiment are highly recommended and widely grown variety for the north-eastern plain zone of India. Kundan is apt for cultivation under rainfed and limited inputs; the variety is a double dwarf, and its height ranges from 80 to 100 cm. This is the only cultivated dwarf variety that has distinct pubescent glumes and highly resistant against rusts and with a life cycle of 135 days. PBW 343 (PAU: Punjab Agricultural University, Ludhiana) is sown under well-irrigated condition, unique in its wide adaptability, a high degree of resistance to rusts (brown and yellow), and tolerance to kernel bunt. The grains are amber, semi-hard to formidable, good straw strength resulting in high yield.

Seed sowing and fertilization doses

Seeds of wheat were manually sown in the field at a rate of 15×30 cm (i.e., the distance between plants were 15 cm and between two row 30 cm) using recommended agronomic practices including fertilizer doses given as urea (120 kg ha^{-1}), superphosphate (60 kg ha^{-1}), and muriate of potash (40 kg ha^{-1}). One-third of N and full doses of P and K were given as basal dressing, and another two doses of N were given as a top dressing after 60 and 90 days of germination. Plants were thinned after 1 week of germination, maintaining a uniform distance of 15 cm. Manual weeding and irrigation were done regularly. There were about 12 plants in each row comprising 145 plants in each plot; the edge of plots was skipped for sowing to reduce edge effect.

Ozone monitoring, AOT40 calculation, and EDU application

Ambient ozone monitoring was carried out by 2B Tech Ozone Monitor (106-L) on an average of 8 hours (9:00 to 17:00) at the experimental site throughout the experiment. The experiment was conducted from November through April. Accumulated Ozone Threshold 40 ppb (AOT40) was calculated for exposure index for ozone, as described by De Leeuw and Van Zantvoort (1997). EDU was kindly provided by Prof. W.J. Manning, University of Massachusetts, USA. Two formulations of EDU were prepared by FAR Research, Inc., Palm Bay, Florida. One formulation was 100% EDU and the other was a 52.5% suspendable powder. Both formulations were chemically verified and certified as pure EDU by R.K.S. WAT, part of the original team that synthesized the EDU at Du Pont in 1975 (Manning et al. 2011). EDU was applied to plants in part per million concentrations (ppm). In the present study, the foliar spray was used for EDU treatment on plants. We selected two EDU concentrations, i.e., 200 and 300 ppm based on a dose-response test (Gupta et al. 2018).

Isolation of apoplast and total soluble protein

Leaves were cut into approximately 5-cm segments and washed with deionized water as rapidly as possible. Segments were vacuum infiltrated for 5 min in 0.2 M KCl, producing a negative pressure of 70 kPa. The pressure was gradually released after 2 min, and the cycle was repeated three times. Segments were then rapidly dried by blotting paper and carefully arranged in a bundle in centrifuge columns (Zeba Desalt Spin Columns, 10 ml, PIERCE). The tubes were centrifuged at 1000*g* for 15 min at 4°C to extract the apoplast solution. The apoplast solution was collected and stored at −20°C for further analysis.

After the apoplastic solution had been extracted, the leaf tissues were ground to powder and extracted with 50 mM HEPES-KOH pH 7.5, 1 mM EDTA, 5 mM DTT, 10% (v/v) glycerol, 2 mM benzamidine, and 2 mM €-aminocaproic acid, stirred for 15 min at 4°C, and centrifuged at 13,000*g* for 15 min at 4°C. The supernatant was used as a total soluble protein for further analysis.

Assay to estimate cytoplasmic contamination in apoplast isolates

The G-6-PDH (glucose-6-phosphate dehydrogenase) enzymatic assay was performed according to the method described by Weimar and Rothe (1987) to check the contamination of the apoplast isolates by cytoplasmic proteins. The following

reaction mixtures were prepared: 170 μl reaction buffer (0.1 M Tris-HCl pH 7.6, containing 12.5 mM $MgCl_2$), 10 μl glucose-6- phosphate (60 mM), and 10 μl nicotinamide adenine dinucleotide phosphates (NADP) (20 mM). The reaction was started by the addition of 10 μl of the concentrated apoplast isolate or total leaf soluble isolate, and the change in absorbance at 340 nm was monitored over 5 min at 25°C using a UV/visible spectrophotometer.

To estimate, cytoplasmic contamination in apoplast, the total leaf soluble proteins were also extracted. Leaf tissues were frozen in liquid N_2 and ground to a fine powder. The powder was suspended in extraction buffer (50 mM HEPES-KOH pH 7.5, 1 mM EDTA, 5 mM DTT, 10% (v/v) glycerol, 2 mM benzamidine, 2 mM Є-aminocaproic acid). After centrifugation (13,000*g* for 15 min at 4°C), the supernatant was used for the G6PDH enzyme assay. Finally, the cytoplasmic contamination was calculated as the percentage of G6PDH activity in the apoplast isolates compared with the activity in the total leaf soluble protein extracts on a fresh weight basis. Three biological replicates for each treatment were made as well as control was taken.

Isolation of intact chloroplast

The method of Navari-Izzo et al. (1998) was followed with some modifications. Thirty grams of fresh wheat leaf was taken and blended into 90 ml of CIB (chloroplast isolation buffer) (330 mM sucrose, 50 mM HEPES-KOH (pH 7.5), 10 mM $MgCl_2$, 10 mM NaCl) then filtered through eight layers of Miracloths (Calbiochem) and centrifuged at 200*g*, 3 min, 4°C. The filtrate was transferred to another 50-ml centrifuge tube (Beckmen, USA), and the chloroplasts were pelleted at 1300*g* for 10 min (Beckman Coulter Avanti Centrifuge J-25, fixed-angle rotor JA- 25.50). The supernatant was decanted, and the pellet was resuspended in 2 ml of resuspension buffer (300 mM sucrose, 50 mM HEPES, 2 mM Na-EDTA, 1 mM $MgCl_2$, and 0.1% BSA). A stepwise Percoll density gradient was assembled by overlaying 10 ml of 80% Percoll in CIB (without BSA) with 10 ml of 40% Percoll in CIB without BSA. Re-suspended pellet was loaded on 40 and 80% of Percoll gradient (Sigma) and centrifuged at 4000×*g*, 10 min, 4°C. Chloroplasts were collected at 40/80% interface and washed in CIB, and the pellet was resuspended by the gentle handshake. A workflow diagram outlining the isolation protocol is given in Fig. S1. Chlorophyll estimation was performed using 0.990 ml of 80% acetone and 10 μl of chlorophyll pellet and incubated for 30 min and centrifuged at 3000*g*, 2 min, 4°C, and the supernatant was read under spectrophotometer at 650 nm, and estimation was performed as per Arnon (1949). All the experiments performed during the isolation of intact chloroplast were carried out at cold room at 4°C to avoid protease activities.

Purity and intactness of chloroplast

The intactness of the chloroplast was estimated by ferricyanide-dependent O_2 evolution (Walker 1980). Assay medium contained 0.33 M sorbitol, 1 mM $MgCl_2$, 1 mM $MnCl_2$, 2 mM EDTA, and 50 mM Hepes-KOH (pH 7.6) for osmotic shock of the chloroplast. To 0.1 ml of chloroplast suspension, 0.9 ml of water was added and allowed to stir for 1 min. Then 1 ml of double-strength assay medium (0.66 M sorbitol, 2 mM $MgCl_2$, 2 mM $MnCl_2$, 4 mM EDTA, 100 mM Hepes-KOH pH 7.6) was added. For assay of the chloroplast intactness, 0.1 ml of chloroplast suspension was added with 1.9 ml of assay medium. Then 10 mM D, L-glyceraldehyde was added with the assay (this inhibits the reductive pentose phosphate pathway (RPPP) and its associated O_2 evolution) along with 3 mM potassium ferricyanide. Two or 3 min after illumination, 5 mM NH_4Cl was added, and rate of light-dependent O_2 evolution (μmol O_2 evolved mg^{-1} Chl h^{-1}) was measured after the addition of NH_4Cl with shocked (A) and unshocked (B) chloroplast. The percent intactness of the chloroplast was calculated as follows:

$$\%\text{intactness} = \frac{\text{A-B}}{\text{A}}(100) = 100\text{-}(100\text{B}/\text{A})$$

Estimating cytoplasmic contamination in isolated chloroplast

After estimation of protein content, 7 μg of protein samples was loaded on 10% SDS-PAGE. Gel was immersed in 100 ml cathode buffer (25 mM tris, 40 mM glycine, 10% (v/v) methanol) for 15 min. Transfer membranes (Immobilon- P, Millipore) were incubated in 100% methanol for 15 s, washed for 2 min in water, and subsequently equilibrated for at least 5 min in 100 ml anode buffer II (25 mM Tris, 10% (v/v) methanol). Six pieces of filter paper (Grade GB003, Whatman) in the size of the membranes were incubated as follows: three in 100 ml cathode buffer, two in 100 ml anode buffer I (0.3 M Tris, 10% (v/v) methanol), and one together with the membrane in 100 ml anode buffer II (filter paper on top and membrane below the paper).

The transfer sandwich was placed and assembled directly on the anode plate of the semi-dry blotting device (Trans-Blot SD Semi-dry transfer cell, Bio-Rad). Assembly of the transfer sandwich from anode to cathode: two filter papers with anode-buffer I, one filter paper with anode buffer II, membrane, separating gel, and three filter papers with cathode-buffer. The transfer was performed at a constant 17-volt, maximum current for 16 h.

Tris-buffered saline tween (TBST) buffer (pH 7.5) containing 1% bovine serum albumin (BSA) was used to block the blotting membrane for 1 h. Membranes were washed five

times: two short immersions, then a 15-min wash followed by two 5-min washing steps. Incubation with primary antibodies was performed at room temperature for an hour, followed by the previously described washing procedure. The final concentration for the primary antibody was 1:3000, 0.25% BSA in TBST buffer.

HRP conjugated cross-reactive secondary antibody (1:20,000 dilutions) in 0.25% BSA containing TBST buffer was used for probing primary antibody for 2 h. Blot was developed with HRP chromogenic substrate (TMB) for 5–10 min to visualize reactive bands.

Protein extraction from chloroplast isolates

Proteins were extracted from frozen chloroplast pellets using chloroplast lysis buffer (7.5 M urea, 2.5 M thiourea, 12.5% glycerol, 62.5 mM tris–HCl, 2.5% n-octyl glycoside, 1.25 mM protease inhibitor) and subsequently precipitated with 10% TCA (trichloroacetic acid) overnight. Next day, after centrifugation, pellet was washed three times with cold acetone and 0.07% β-ME. The pellet was then vacuum dried, solubilized in 0.1 M Tris-HCl (pH 8.0), 50 mM EDTA, and 2% β-ME. Proteins were extracted with 2.5 mL Tris-buffered phenol. Ten milliliter, 0.1M ammonium acetate in methanol was added to the phenol phase and left overnight at −20°C. The next day, after centrifugation, pellet was dissolved in 0.1M ammonium acetate in methanol and 1% β-ME and then washed twice with cold acetone and 1% β-ME. Now, the dried pellet was resuspended in a solubilization buffer consisting of 7 M urea, 2 M thiourea, 2% CHAPS, 20 mM DTT, and 0.5% v/v immobilized pH gradients buffers. The composition of lysis buffer was designed in such a way that it helped to break the chloroplast membrane, thylakoid membrane, easing to extract the protein inside. We have tried to extract all the possible chloroplast proteins, either it is from stroma, lumen, and thylakoid. Protein estimation was carried out according to Bradford's (1976) method with bovine serum albumin (BSA, Sigma) as standard, and absorbance was measured at 595 nm.

Protein separation by SDS-PAGE in apoplast and chloroplast isolates

Samples were prepared for SDS-PAGE in 1X loading buffer, and protein samples were loaded on stacking gel with 2X gel loading buffer (for 1X: 50 mM Tris-HCL, 2% SDS, 10% [v/v] glycerol, 0.05 M DTT, and 0.1% bromophenol blue). Electrophoresis was carried out on polyacrylamide slab gels (60 mm×80 mm×1 mm), using the discontinuous buffer system. The 5% stacking gel was overlaid on the separating gel of 12% polyacrylamide with an acrylamide: Bis ratio of 29:1. Electrophoresis was performed in a standard Tris-Glycine running buffer in a Miniprotein III dual slab cell (Bio-Rad) at a constant 70 V slab gel using a Power PAC300 (Bio-Rad).

Gels were stained with 0.5% coomassie brilliant blue G and destained with 10% glacial acetic acid in 50% methanol, and images were acquired with a document scanner. Image analysis was performed using Image Quant TL 7.0 software (GE Health care). The criteria for defining the protein abundance patterns were determined as follows: upregulated, % volume increased at least one- and half-fold; downregulated, % volume decreased at least one- and half-fold; unchanged, % volume varied within one- and half-fold.

2D-PAGE (two-dimensional polyacrylamide gel electrophoresis) of chloroplast protein

Two-dimensional gel electrophoresis (2-DGE) was carried out as described in Lehesranta et al. (2005) with some modifications. Protein samples (120 μg) were rehydrated overnight on immobilized pH gradients (IPG) strips (7 cm, pH 4–7, linear) with 135 μl of rehydration buffer (7 M urea, 2 M thiourea, 2% CHAPS, 20 mM DTT, 0.5% v/v immobilized pH gradients buffers) in a reswelling tray (Amersham Biosciences, Uppsala, Sweden) at room temperature. Isoelectric focusing (IEF) was conducted at 20°C with an Ettan IPGphore-3 (GE Healthcare) and a Dry Strip kit (Amersham Biosciences, Uppsala, Sweden). The operating conditions were as follows: 250V for 1 h, 500V for 1 h, 1500V for 2 h, 4000V for 2 h, and 6000V for 2 h for a total of 21.2 kVh. The focused strips were equilibrated twice for 10 min in 5 mL of equilibration solution (6M urea, 30% w/v glycerol, 2% w/v sodium dodecyl sulfate (SDS), and 50 mM Tris-HCl buffer, pH 8.8). The first and second equilibration buffer only differed in having either 1% w/v DTT or 2.5% w/v iodoacetamide. Electrophoresis was carried out on polyacrylamide slab gels (60 mm×80 mm×1 mm), using the discontinuous buffer system. The separating gel of 12% polyacrylamide with an acrylamide: Bis ratio of 29:1 was used. Electrophoresis was performed in a standard Tris-Glycine running buffer in a Miniprotein III dual slab cell (Bio-Rad) at a constant voltage of 70V and 120V using a Power PAC300 (Bio-Rad). Three gel replications were performed. To visualize the protein spots, the PAGs were stained with Sypro ruby (Sypro-ruby staining kit, Sigma-Aldrich). The data were analyzed using Image Master 2D Platinum 7.0 (IMP 7) software (Amersham Bioscience). IMP 7 automatically performed statistical analysis among control and EDU treatments ($P< 0.05$) to measure significant differential expression. Relative volume (% volume) was used to quantify and compare the spots. The relative volume considers the ratio of detected spot pixel density to the sum of all analyzed spot pixel density. Hence, this procedure permitted to normalize experimental variations due to protein loading and staining. Three gels of each sample were considered in order to obtain a sample replicate set. The criteria for defining the protein

abundance patterns were determined as follows: upregulated, % volume increased at least one- and half-fold; downregulated, % volume decreased at least one- and half-fold; unchanged, % volume varied within the range of one- and half-fold.

Protein identification

Tryptic digestion of protein spots excised from the gels and sample preparation were performed according to Koistinen et al. (2002). Briefly, gel particles were destained and dehydrated by washing three times with 25 mM ABC (ammonium bicarbonate) containing 50% acetonitrile. Destained particles were dried in a vacuum centrifuge concentrator and rehydrated in equal volumes of 0.1 mg ml^{-1} trypsin and 50 mM ABC. Gel particles were immersed in 25 mM ammonium bicarbonate, and samples were digested overnight at 37°C. Peptides were extracted twice with 50% ACN/1% TFA, gel particles were rehydrated with water, and two more extractions were performed. The recovered peptides were concentrated to a final volume of 20 μl. The extracted peptides were desalted and concentrated for MALDI analyses using C 18 Zip Tips (Millipore, Schwalbach, Germany).

MS and MS/MS

A 4800 Proteomics Analyzer (Applied Biosystems) with TOF/ TOF optics was used for all MALDI-MS and MS/MS applications. Samples were prepared by mixing 0.5 ml of sample with 0.5 ml of matrix solution (5 mg/mL a-cyano-4-hydroxycinnamic acid in 50% ACN containing 0.1% TFA) and spotted on stainless steel 384-well target plate. They were allowed to air dry at room temperature and then inserted in the mass spectrometer and subjected to mass analysis. The mass spectrometer was externally calibrated with a mixture of angiotensin I (m/z 1296.685), Glu-fibrinopeptide B (m/z 1,570.677), ACTH clip (1–17) (m/z 2093.086), and ACTH clip (18–39) (m/z 2465.199). For MS/MS experiments, the instrument was externally calibrated with a fragment of Glu-fibrinopeptide B. The monoisotopic peptide masses obtained from MALDI-TOF/TOF were analyzed by the 4000 Series Explorer software version 3.5 (ABI). On the basis of mass signals, protein identification was performed with the Mascot software (http://www.matrixscience.com) to search proteins against Swiss Prot, NCBInr, and MSDB databases. The following parameters were used for database searches: monoisotopic mass accuracy, <100 ppm; missed cleavages, 1; carbamidomethylation of cysteine as fixed modification and oxidation of methionine, N-terminal pyroglutamylation (peptide), and N-terminal acetylation (protein) as variable modifications.

Results

Meteorological conditions and ambient ozone

A dry tropical monsoon climate characterizes the weather of Lucknow. Average maximum temperatures varied from 20 to 39°C, and the average minimum temperature varied from 9 to 27°C during the whole year. Mean sunshine hours were least in December while maximum in April. Meteorological parameters during the experimental period are provided in Table S1.

Ambient average ozone concentration during the experiment was 60 ppb (Table 1). Its concentration was variable because of the variable weather conditions. It has been shown that precipitation and cloudy weather are responsible for low ambient ozone due to the washout of tropospheric ozone and lack of sunlight. In the month of November, December, and March, ozone was higher than in January and February (Fig. 1).

Apoplast isolation and its purity

The intracellular contamination levels in the vacuum infiltrated apoplast (VIA) were quantitatively evaluated from the enzyme activity of glucose-6-phosphate dehydrogenase (G6PDH). On this basis, contamination of VIAs with other intracellular proteins appeared negligible. The average contamination percentage was 1.24%, 2.93%, and 1.45% for the KCON, K-200, and K-300, while for PCON, P-200, and P-300, it was 2.18%, 1.53%, and 2.53%, respectively (Fig. S2).

Chloroplast isolation, intactness, and its purity

The isolation of chloroplast was done using a Percoll gradient method. The chloroplast's intactness was found to be in the range 85–90% as estimated by ferricyanide-dependent O_2 evolution. Light microscopy reconfirmed (data not shown) the intactness of isolated chloroplasts.

Western blot analysis was performed to detect cytoplasmic impurities in the isolated chloroplast fraction against a readymade antibody of UGPase (UDP-glucose pyrophosphorylase) E.C. = 2.7.7.9., a cytoplasmic protein from goat (cytoplasm marker) (Fig. 5) (Agrisera). Immunoblots showed that the chloroplasts were free of contamination by cytoplasm (Fig. 5A and B). Lanes 2 and 3 showed negligible expression of cytoplasmic UGPase against positive control (lane 4) of total soluble protein (rice). These results demonstrate that the chloroplasts are highly import-competent and that their envelope membranes are intact.

Table 1 Average ozone concentration (ppb) and AOT 40 (ppm.h) during different developmental stages of wheat

Stages	Germinating stages	Vegetative stages	Flowering stages	Maturation stages
Avg Ozone (ppb)	58.90	41.84	63.13	75.13
AOT 40 (ppm.h)	5.44	0.52	6.66	10.11

Proteomic analysis

SDS-PAGE analysis for apoplast isolates

Image quant analysis result shows significant differentially abundant protein bands in the gel ($P< 0.05$). The image quant software detected twenty-six bands at the vegetative stage in each lane. Out of these 26 protein bands detected, 10 (K1), 12 (K2), 6 (P1), and 8 (P2) protein bands showed a differentially abundant response. The protein expression pattern, i.e., 8 (K1) and 2 (K2) protein bands, increased whereas 8 (K1) and 4 (K2) decreased in their expression under EDU treatment. On the other hand, 2 (P1) were more abundant and 4 (P1) were less abundant, whereas 2 (P2) increased, and 6 (P2) decreased in their expression under EDU treatments (Fig. 2A). In the flowering stage (16–26) bands were detected by the image quant software in each lane. The image quant analysis showed, 9 (K1), 10 (K2), 14 (P1), and 14 (P2) protein bands were differentially expressed under EDU treatment. Out of 16 proteins in Kundan, 7 protein bands were more abundant and 2 less abundant in K1 while 10 (K2) showed only increased abundance, respectively. In PBW343, 13 protein bands were more abundant, and 1 was less abundant (P1), whereas 8 increased and 6 protein bands were less abundant in P2 under EDU treatments (Fig. 2B).

In Kundan variety, catalase, amino methyltransferase (AMT), serine glyoxylate aminotransferase (SGAT), and superoxide dismutase (SOD) proteins were more abundant at both stages whereas, in PBW 343, Germine-like protein, SOD, and thioredoxin-dependent peroxidase (TPX) were also more abundant at both developmental stages under two doses of EDU (Tables 2, S2, and S3). In Kundan, Germin-like protein was less abundant at both stages, whereas, in PBW 343, catalase, AMT, SGAT, ascorbate peroxidase (APX), and TPX were less abundant at both developmental stages under EDU treatment (Tables 2, S2, and S3).

SDS-PAGE analysis for chloroplast proteins

Image quant analysis results of extracted chloroplast proteins showed a significant differential abundance of protein bands in the brilliant blue stained reference gel ($P< 0.05$) (Fig. 3). Image Quant TL 7.0 software detected (20–25) protein bands in each lane. Out of detected protein bands 8 (K1), 6 (K2), 5 (P1), and 16 (P2) number of bands were differentially abundant under EDU treatment, respectively. In Kundan, 3 and 5 bands (more abundant) in K1, whereas in K2, 5 and 1 bands (less abundant) were found to be differentially expressed under EDU treatment. On the other hand, in P1, 3 protein bands were more abundant, and 2 were less abundant, while in P2, all 16 bands were more abundant under EDU treatments (Fig. 3).

2D-PAGE analysis for chloroplast proteins

Three representative gels were analyzed for each treatment with each variety (Fig. 4). In total, more than 332 protein spots were reproducibly detected on Sypro ruby–stained gels within each treatment in Kundan, whereas in PBW 343, 283 spots were reproducibly detected. Several significantly differentially abundant proteins ($P < 0.05$) were observed under EDU treatment in both the varieties. In Kundan, out of 332 spots, 164 spots were matched to all the gels. In K1, 39% were increased, 19% were decreased, and 42% showed no change, whereas, for K2, more abundant protein spots were found to be 22% whereas 25% spots were less abundant while 53%

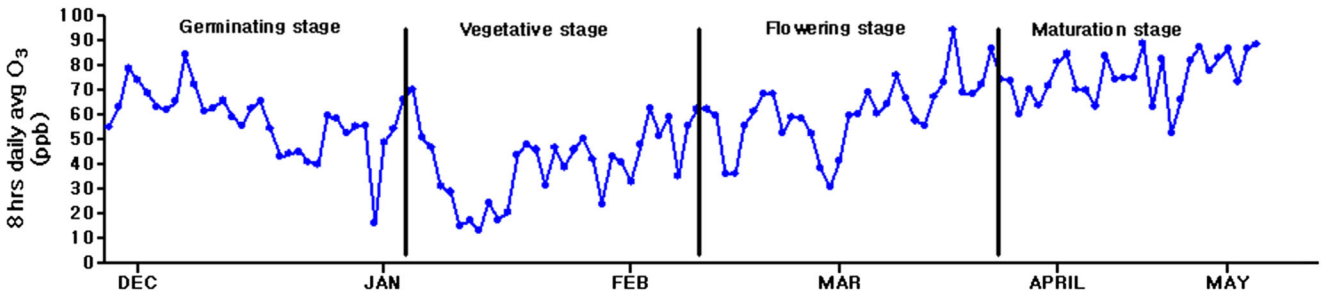

Fig. 1 Daily ozone concentrations (8 h average) during the study period (November–April). The different stages for wheat growth are shown in colored boxes, and dots denote the date of the month

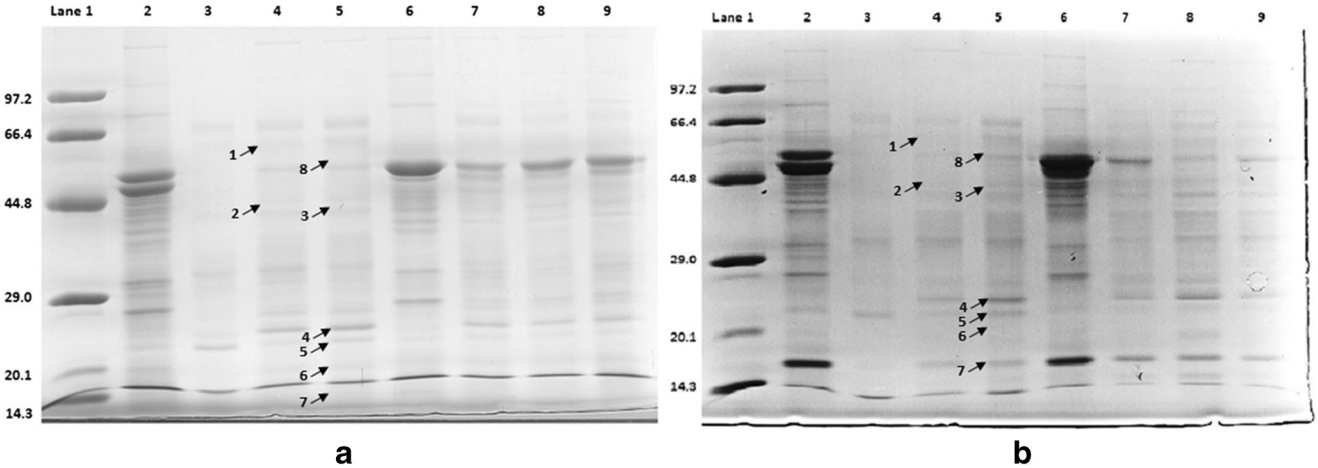

Fig. 2 Effect of EDU on Apoplast protein in two wheat varieties Kundan and PBW 343 leaves at vegetative (A) and flowering stages (B). (12% gel, 25 μg protein loading) Brilliant blue G–stained SDS-PAGE gel representing molecular marker (lane 1, in kDa), total leaf protein (lanes 2 and 6), Apoplast protein control (lanes 3 and 7), 200 ppm EDU dose (lanes 4 and 8), and 300 ppm EDU dose (lanes 5 and 9) in Kundan and PBW 343, respectively. Proteins were identified by mass spectrometry, and protein numbers were adopted from Table 2; for details, see "Materials and methods"

showed no change as compared to their respective controls (Fig. S3 (A, B, C, and D)). On the other hand, out of 283 spots in PBW 343, 221 spots were matched to all the gels. The more abundant protein spots were found to be 12% whereas 25% were less abundant while 63% showed no change in P1 compared to their respective controls. For P2, 28% were more abundant, 27% were less abundant, and 45% showed no change under EDU treatment.

These identified proteins were categorized into different functional categories, as shown in Fig. S4 (A and B). There were 7 protein categories based on their biological functions related to photosynthesis, carbon metabolism, and energy metabolism, and a differential abundance of proteins under EDU treatment in both varieties. The protein synthesis assembly and degradation (PSAD) functional category has a maximum of 11 proteins differentially expressed under EDU treatment. Some of the proteins related to amino acid metabolism, defense, and redox signaling also have their roles in EDU-induced signaling effects in chloroplast proteome (Table 3). Their roles in

Table 2 List of EDU-responsive apoplast proteins in two wheat varieties, i.e., Kundan and PBW 343 at two different developmental stages analyzed from SDS-PAGE and identified by mass spectrometry (MS). Values (mean of three replicate gels within each treatment) represent fold changes with threshold of 1.5-fold increased or decreased. (↑) denotes increased expression of proteins; (↓) denotes decreased expression of proteins; (-) denotes no change

Protein. no.	Protein names	Functions[A]	Kundan, vegetative stage		Kundan, flowering stage		PBW 343, vegetative stage		PBW 343, flowering stage	
			200 ppm	300 ppm	200 ppm	300 ppm	200 ppm	300 ppm	200 ppm	300 ppm
1	Catalase	H_2O_2 catabolism	1.77↑	2.64↑	-	2.28↑	-	−1.86↓	2.02↑	−8.15↓
2	Aminomethyl transferase	Transaminase activity	6.18↑	-	2.46↑	−4.11↓	−2.32↓	1.71↑	−3.32↓	−1.60↓
3	Serine-glyoxylate aminotransferase	Transamination	3.91↑	7.58↑	-	6.68↑	−1.66↓	2.76↑	−1.70↓	-
4	2-Cys peroxiredoxin	Response to stress	2.49↑	-	8.93↑	14.44↑	1.72↑	-	4.02↑	1.89↑
5	Germin-like protein	Nutrient reservoir	−1.50↓	1.68↑	−5.58↓	4.67↑	−2.19↓	2.81↑	-	3.28↑
6	Cu/Zn superoxide dismutase	First line of defense	4.27↑	4.29↑	8.12↑	7.83↑	−1.54↓	-	13.91↑	2.50↑
7	L-ascorbate peroxidase	Defense response	-	-	-	-	-	−1.98↓	1.50↑	−2.10↓
8	Thioredoxin-dependent peroxidase	Cell redox homeostasis	-	-	-	-	-	−5.27↓	-	2.03↑
9	Unnamed protein product	-	2.70↑	5.54↑	-1.94↓	1.58↑	1.69↑	1.94↑	7.79↑	5.83↑

[A] Functions of the proteins as per" www.uniprot.com"

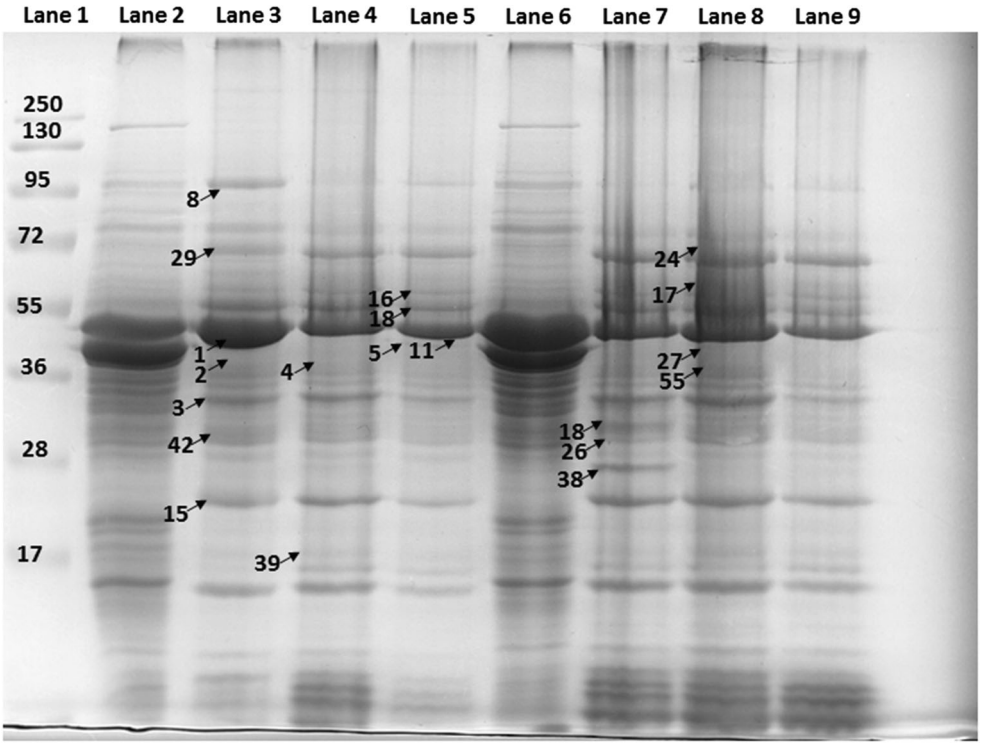

Fig. 3 Initial evaluation effect of EDU on the wheat chloroplast proteome. SDS-PAGE profiling of wheat chloroplast proteins. Total soluble proteins were separated by 12% SDS-PAGE. Both varieties were extracted in parallel and separated proteins (60μg/lane) were stained with colloidal CBB G-250. Lane 1, molecular weight marker (5 μL of the Prestained Protein Standards, Thermo scientific); lane 2, total soluble protein of z; lane 3, control of Kundan; lane 4, 200 ppm EDU of Kundan; lane 5, 300 ppm EDU of Kundan; lane 6, total soluble protein of PBW 343; lane 7, con of PBW 343; lane 8, 200 ppm EDU of PBW 343; lane 9, 300 ppm EDU of PBW 343. Protein numbers were adopted from the Table 3

EDU-mediated signaling and functions have been shown in Tables 3, S4, and S5.

Discussion

To investigate EDU's mode of action, apoplast and chloroplast isolate proteome profiling was done using 1D/2D PAGE with two EDU concentrations under high ambient ozone. Isolation of apoplast and chloroplast were performed from the fresh leave of two wheat varieties. Two EDU concentrations 200 and 300 ppm were used based on the prior standardized protocol in wheat (Gupta et al. 2018). The EDU approach assumes that this chemical alleviates ozone effects on crops while having no constitutive effects on plants (Ashrafuzzaman et al. 2017).

Meteorological conditions and ambient ozone

At the experimental site (Lucknow, India), the maximum average temperature was recorded during March, whereas the minimum average temperature was recorded in January. Mean hourly average ozone concentrations of 60 ppb (more than the threshold value of 40 ppb) during the experimental period was enough to cause phytotoxicity. This caused substantial injury to the wheat leaves (Gupta et al., 2018). Above 40 ppb of ozone can cause detrimental injuries in plant leaves (Singh et al. 2010). Maximum ozone concentrations were recorded in the maturation stage (78 ppb), and the minimum was recorded near to the threshold value in January (ca 38 ppb). These concentrations are in line with several other measurements nearby the Lucknow area in India, as reviewed in Oksanen et al. (2013).

Role of apoplast proteins in EDU protection

To investigate plant apoplast protein role in EDU protection, it was important to isolate and identify their role in specific antioxidative defense processes. The cytoplasmic contamination in apoplast isolate was quantitatively evaluated from the activity of glucose-6-phosphate dehydrogenase (G6PDH) enzymatic assay (Weimar and Rothe 1987). The apoplast isolates contained negligible cytoplasmic contamination (< 3%) in both the varieties and EDU treatments. According to previous studies, less than 3% cytoplasmic contamination is permissible in apoplast isolates (Alves et al. 2006). This cytoplasmic enzyme can be used as a specific marker for any plasma membrane damage that may occur during apoplast extraction by the vacuum infiltration procedure (Vanacker et al. 1998). Ozone phytotoxicity is believed to be due to loss of membrane integrity and ROS formation in the apoplast (Heath 1988). We report nine apoplastic proteins involved in different physiological and defense functions under EDU treatment in two wheat varieties (Tables 3, S2, and S3).

Catalase (protein no. 1) was more abundant in Kundan under EDU treatment showing its involvement in defense mechanism under prevailing ozone concentration. Catalase was increased in both K1 and K2 at both developmental

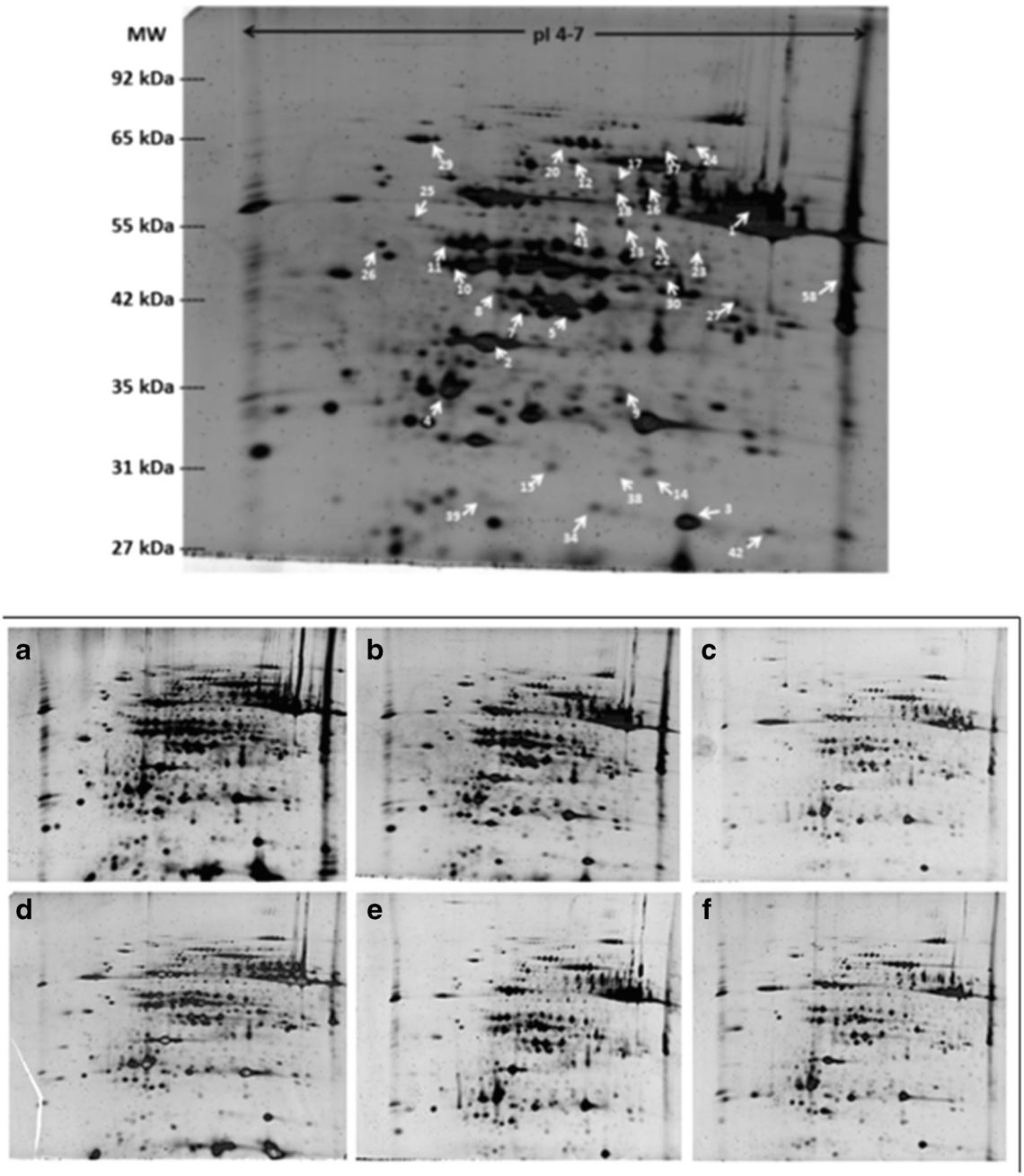

Fig. 4 Effect of EDU application on chloroplast proteome of two wheat varieties Kundan, and PBW 343 leaves with two EDU treatment. (12% gel, 120 μg loading, pH range 4–7, Sypro ruby stained two-dimensional gel representing control (A, D), 200 ppm EDU treatment (B, E), and 300 ppm EDU treatment (C, F). The arrows indicate in reference gel proteins identified by mass spectrometry, for details, see "Materials and methods." A, B, C = Kundan and D, E, F = PBW 343

stages. Increased activity of catalase in Kundan depicts ROS scavenging and EDU-induced protection. Similar results were also reported in EDU-treated *Phaseolus vulgaris* L. leaf (Brunschon-Harti et al. 1995). In PBW 343, catalase abundance was differential with decreases in P2 at both the developmental stages depicting less EDU protection. It has been reported that ozone exposure enhances the defense-related antioxidative enzymes in the wheat apoplast (Wang et al. 2014).

SOD (protein no. 5) increased in Kundan and differentially expressed in PBW 343 in apoplast isolate under EDU treatment. Involvement of SOD for scavenging ozone-induced ROS has been reported by several workers (Sarkar et al. 2010; Willick et al. 2018). The activity of SOD was increased in K1 and K2 at both the development stages. SOD is the first line of defense to cope with oxidative burst under ambient ozone stress (Singh and Agrawal 2010). Its abundance in apoplast isolate reveals EDU protection even at the

Table 3 List of EDU-responsive chloroplast proteins in two wheat varieties, i.e., Kundan and PBW 343 at two different developmental stages using two-dimensional gel electrophoresis (2D-GE) and identified by mass spectrometry (MS). Values (mean of three replicate gels within each treatment) represent fold changes with threshold of 1.5-fold increased or decreased. *LSU*, large subunit; *SSU*, small subunit; (↑) denotes increased abundance of proteins; (↓) denotes decreased abundance of proteins; (-) denotes no change

S. no.	Protein names	Functions[A]	Kundan		PBW 343	
			200 ppm	300 ppm	200 ppm	300 ppm
Photosynthesis related proteins						
1	Rubisco LSU	RubP carboxylase/oxygenase activity	1.68↑	2.14↑	−1.93↓	−2.45↓
2	Oxygen evolving enhancer protein	PS II Regulation	1.75↑	−1.64↓	1.52↑	1.60↑
3	Cyt-b6f complex	Electron transport	-	-	1.75↑	2.22↑
4	a/b- binding protein	Light harvesting	1.92↑	2.15↑	-	-
5	Ferredoxin dependant- NADP(H) reductase	Electron transport	2.92↑	2.33↑	2.13↑	3.44↑
6	Crystal Structure of Psbp	Quenching	−2.14↓	-	2.61↑	1.66↑
Carbon netabolism proteins						
7	Rubisco activase (chloroplastic)	ATP binding	1.54↑	-	-	−2.56↓
8	Hydrolase	Epoxide hydrolase activity	-	-	1.97↑	−3.57↓
9	Triosephosphate isomerase	Carbohydrate metabolism	1.78↑	1.79↑	1.92↑	−4.50↓
10	Phosphoribulo kinase	ATP binding	-	-	-	−2.48↓
11	Fructose bisphosphate aldolase	Glycolytic Process	2.67↑	1.82↑	−1.55↓	−2.61↓
12	Enolase	Glycolytic Process	-	-	3.44↑	3.51
13	Glyceraldehyde-3-phosphate dehydrogenase	Oxidoreductase activity	−5.34↓	−1.97↓	−1.88↓	−1.55↓
14	Ribose phosphate isomerase	Ribose metabolism	1.60↑	-	-	−2.28↓
Energy metabolism related proteins						
15	Peroxiredoxin	Peroxidase activity	-	-	−2.47↓	-
16	ATP synthase α- subunit	ATP synthesis	−2.15↓	−2.08↓	2.63↑	3.67↑
17	ATP synthase β- subunit	ATP synthesis	−4.30↓	−2.12↓	−1.97↓	−2.66↓
18	ATP synthase ε- subunit	ATP synthesis	−1.96↓	−1.87↓	1.65	-
19	Adenosine diphosphate glucose pyrophosphatase	Starch synthesis regulation	-	-	1.78↑	1.59↑
20	Vacuolar proton ATPase	Proton pump	−4.30↓	-	-	-
21	Aminomethyl transferase	Transaminase activity	-	-	-	1.81↑
22	F0-F1 ATPase alpha subunit	ATP synthesis	−3.63↓	−1.75↓	-	2.24↑
Protein synthesis assembly and degradation						
23	Rubisco LSU binding protein (α and β)	Protein refolding	-	−2.44↓	1.75↑	-
24	Cheperone protein ClpC2	Protein metabolism	-	-	2.91↑	2.16↑
25	Trigger factor	Protein folding/ transport	−3.38↓	1.58↑	-	2.40↑
26	30S Ribosomal protein	Protein synthesis	1.79↑	1.74↑	1.65↑	1.84↑
27	20Kda chaperonine	Protein folding	1.53↑	-	2.03↑	-
28	ATP dependatnt clp protease binding protein	Protein unfolding	-	−2.42↓	-	-1.83↓
29	70Kda heat shock protein	Stress response	−2.05↓	−1.77↓	-	1.66↑
30	Elongation Factor	Translation elongation	−1.97↓	-	-	−1.53
31	Eukaryotic initiation factor 4A	Translation initiation	−1.67↓	-	4.27↑	3.10↑
32	Peptidyl-prolyl cis-trans isomerase	Cis-trans interconversion	1.58↑	2.66↑	−1.62↓	1.58↑
33	ATP-dependent zinc metalloprotease	Membrane catabolism	2.07↑	1.87↑	−1.61↓	1.65↑
Amino Acid metabolism						
34	Thioredoxin H-type 4	Cell redox homeostasis	−1.61↓	−2.00↓	2.38↑	−2.42↓
35	cp31BHv	RNA- binding	−2.12↓	−2.17↓	1.75↑	1.66↑
36	Glutamine synthetase	Glutamine synthesis	1.64↑	−1.56↓	-	−1.75↓
37	Glycine dehydrogenase	Glycine cleavage	-	-	-	2.60↑
Defense						
38	Germin like protein	Nutrient reservoir	−1.75↓	1.51↑	−1.89↓	-
39	L-Ascorbate peroxidase	Defense response	-	-	-	−3.95↓

Table 3 (continued)

S. no.	Protein names	Functions[A]	Kundan		PBW 343	
			200 ppm	300 ppm	200 ppm	300 ppm
Cytoskeleton						
40	Translationally controlled tumor protein	Strength to cell	3.18↑	1.89↑	-	-
41	Plastid-lipid-associated protein	Cell membrane formation	-	-	-	−1.77↓
Redox signaling						
42	Nucleoside diphosphate	NDP kinase activity	-	2.13↑	3.40↑	1.63↑

intermembrane space level. O_3-induced oxidative products were found at leaf level in rice and wheat apoplast (Wang et al. 2013, 2014) (Fig. 5). Similar results were also reported in snap bean by Lee and Chen (1982) and Brunschon-Harti et al. (1995). SOD is a major scavenger of superoxide, and its enzymatic action results in the formation of H_2O_2 (Barcelo et al. 2003). In PBW 343, SOD abundance was differential, P1, P2 (less abundance) at the vegetative stage, whereas P2 (more abundance) at the flowering stage. Altered response in PBW 343 may be due to its less responsivity to EDU. As SOD is considered the first line of defense, Kundan better protected itself by increased SOD activity.

Amino methyltransferase (AMT) (protein no. 2) and SGAT (protein no. 3) proteins showed similarly increased abundance in K1 and K2 at both stages, whereas decreases in P1 and P2 (vegetative stage) and (P1) more abundance at the flowering stage. AMT activity generally increases during abiotic stress (Mostek et al. 2016), and overexpression of the SGAT gene was reported by Yang et al. (2013) during salt stress in *Arabidopsis*. AMT transfers the methyl group during protein translation, and SGAT catabolizes asparagine metabolism during photorespiration. During ozone stress, defense-related proteins are more needed. To fulfill this demand, EDU enhanced the abundance of AMT and SGAT in Kundan variety. It showed that Kundan was more EDU responsive under prevailing ozone than PBW 343. Germin-like protein (protein no. 4) was found less abundant in K1 and K2 at both developmental stages. This protein is induced in multiple stresses (Agrawal et al. 2002) and is shown to inhibit serine proteases in the wheat apoplast (Segarra et al. 2003). The decreased activity of protein no. 4 in Kundan was quite interesting for us because it was not expected under EDU treatment. Its more abundance was recorded in P1 and P2 at the flowering stage. This shows that for this protein, EDU protection was more in PBW 343, leading to inhibition of serine proteases under prevailing ozone level. Germin was first described in sprouting wheat grain as an apoplastic, multimeric (130 kDa), and glycosylated enzyme with resistance to heat,

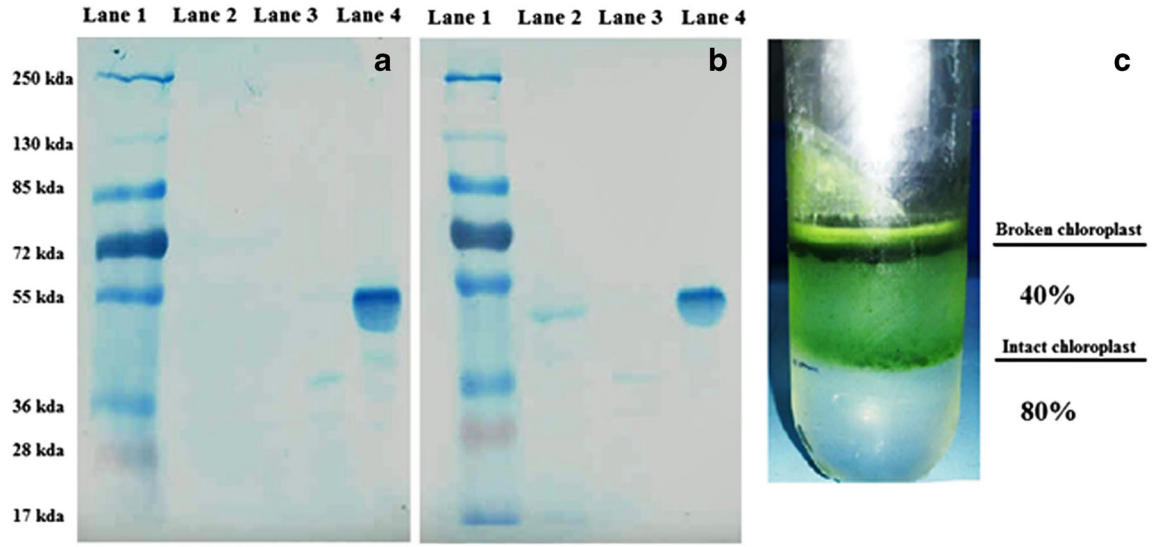

Fig. 5 Western blot analysis of chloroplast protein. Lane 1 represents molecular weight marker, lanes 2 and 3 represents chloroplast proteins, and lane 4 represents positive control, i.e., total soluble protein (rice) in plate A and plate B, respectively. C represents intact chloroplast at 40–80% Percoll interface and broken chloroplasts were accumulated at the top of 40% Percoll

H_2O_2, and proteolysis (Thompson and Lane 1980; Dunwell et al. 2000).

Thioredoxin-dependent peroxidase (TPX) (protein no. 7) was only identified in PBW 343 with differential abundance. TPX abundance was less at the vegetative stage whereas more at the flowering stage with 200 EDU treatment. EDU protected P1 at the flowering stage from ROS produced in apoplast during high ambient ozone. The role of TPX is to protect the molecular mechanism of the cell from the adverse effects of ROS (Goyer et al. 2002). It can be summarized that EDU influenced some important apoplast proteins. We assume that EDU enters the apoplast through stomata and induced some signaling molecule (unknown). This EDU-mediated signaling triggers some other proteins involved in ozone stress coping mechanism, for instance, SOD, CAT, AMT, and SGAT. A model is proposed depicting the role of EDU-mediated changes in apoplast signaling and defense mechanism (Fig. 6). In apoplast, increased SOD and CAT activity reduces the ozone-mediated ROS burst. TRX maintains cell redox homeostasis inside the cell. Overall antioxidative defense and cell homeostasis lead to better ozone stress protection mediated by EDU (Fig. 6).

Role of chloroplast proteins in EDU protection

Analysis of the protein abundance pattern in chloroplast isolates can provide a better molecular explanation of how EDU impacts photosynthetic mechanisms under prevailing O_3 stress (Tables 3, S4, and S5). Several chloroplast proteins involved in different functions were identified by mass spectrometry in the present experiment. It included photosynthesis, carbon metabolism, protein synthesis assembly degradation, defense, and energy metabolism–related proteins (Fig. S3). Prevailing tropospheric ozone and given EDU doses were enough to impact changes in chloroplast protein abundance.

Photosynthesis-related protein like Rubisco LSU (protein no.1) was found with differential abundance in Kundan and decreased in PBW under both the EDU treatments. Rubisco is the most abundant protein in the plant system and has a major role in photosynthesis. Adverse effects of ozone on Rubisco have been reported in several studies (Agrawal et al. 2002; Cho et al. 2008; Sarkar et al. 2010). Less impact of EDU on Rubisco reflected that photosynthesis machinery is not significantly affected by EDU (Pandey et al. 2014; Gupta et al. 2018, 2020). Differential abundance of Rubisco was also shown under EDU treatment in wheat leaf (Gupta et al. 2018) and maize leaf (Gupta et al. 2020). OEE (protein no.

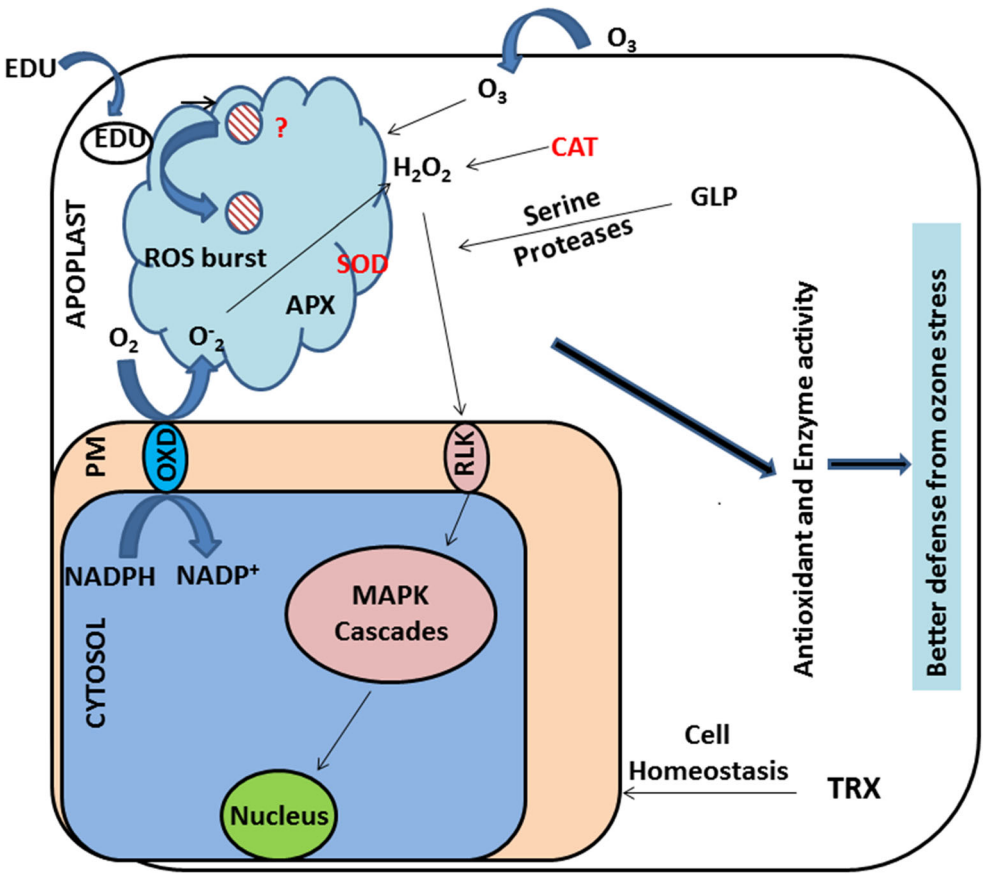

Fig. 6 A proposed model and schematic representation of EDU-mediated signal transduction in apoplast, plasma membrane and cell. CAT, catalase; SOD, superoxide dismutase; GLP, germin like proteins; TRX, thioredoxin dependent peroxidase; OXD, oxidase; RLK, receptor like protein kinase; APX, ascorbate peroxidase; PM, plasma membrane. (red color represents increased expression, and blue represents differential expression)

2) showed a differential response in Kundan, whereas it was increased in PBW 343 at both EDU concentrations. OEE maintained PS II homeostasis during the light reaction in PBW 343 under EDU treatment. Torres et al. (2007) and Bohler et al. (2007) reported a decreased abundance of OEE under higher O_3 exposure. Increased OEE abundance in PBW 343 also showed that the PSII system was protected by EDU, as OEE is also shown as an excellent antioxidant (Kim et al. 2015). Cytochrome b-6-f complex (protein no. 3) was only identified in PBW 343 and was more abundant at both the EDU treatments. Cyt-b6f complex, which contributes to photoprotection and PS II integrity, increased in its abundance showing EDU-mediated protection in PBW 343. It was not identified in Kundan, and we predict this protein may have shown a similar response as in PBW 343. Light-harvesting a/b binding protein (protein no. 4) was more abundant in Kundan with both the EDU concentrations. Increased abundance of a/b binding protein in Kundan showed better EDU protection of the "reaction center" under prevailing ozone stress. FNR (protein no. 5) was increased in Kundan as well as PBW 343 with both the EDU treatments. In chloroplasts, FNR functions as electron carriers in the photosynthetic electron transport chain and as electron donors to various cellular proteins, such as glutamate synthase (Lea-Smith et al. 2016). An enhanced abundance of FNR exhibited an efficient functioning of photosynthetic machinery under better EDU protection. The crystal structure of Psb p (protein no. 6) was decreased in K1, whereas it was increased in P1 and P2. It is involved in the photolysis of water by assisting PS II. Its decreased activity in Kundan was quite interesting for us, but its performance was better in PBW343 with both the EDU treatments. Based on the abundance of proteins related to photosynthesis, it can be said that EDU treatment resulted in limited damage to photosynthetic proteins in both wheat varieties, thereby maintaining optimum photosynthesis under prevailing O_3 stress.

Rubisco activase (protein no. 7) was increased in K1 and decreased in P2. Rubisco activase is required to activate Rubisco to perform its catalytic activity during carbon assimilation (Portis et al. 1986). Its increased activity in Kundan depicts better assistance for Rubisco under EDU treatment. TPI (protein no. 9) was increased in Kundan at K1 and K2 whereas it had a differential response in PBW 343. TPI has a role in carbon metabolism along with starch biosynthesis. Its increased abundance may have provided higher biomass to Kundan under EDU treatment, as we have reported in our previous study (Gupta et al. 2018). TPI may transport out of the chloroplast leading to decreased availability of substrates for energy production and tissue synthesis through glucose catabolism (Bohler et al. 2007). PRK (protein no. 10) and Enolase (protein no. 12) were decreased in abundance except Enolase in P1 (increased). Decreased abundance of PRK and Enolase suggests less EDU protection in PBW to ozone stress. FBPase (protein no. 11) had increased abundance in Kundan and was decreased in PBW with both the EDU treatments. Induction in FBPase increases the carbon fixation in Kundan as it is an integral part of the Calvin cycle (Sarkar et al. 2010). In our previous study, we have reported that Kundan allocated more biomass under EDU treatment (Gupta et al. 2018).

Enhancement of carbon catabolism/metabolism-related enzymes and proteins lead to the change in starch content during O_3 stress (Ahsan et al. 2010). GAPDH (protein no.13) was less abundant in both the varieties and treatment. GAPDH is an integral part of the Calvin cycle and effectively control starch biosynthesis. Reduction in their abundance was not expected and may have altered photosynthesis under EDU treatments in both varieties. RPI (protein no. 14) was increased in K1 and decreased in P2, indicating enhanced carbon metabolism in Kundan over PBW. It has a vital role in the Calvin cycle and the pentose phosphate pathway. It converts ribose-5-phosphate to Ribulose-5-phosphate in the Calvin cycle with the final product of starch or cellulose, which may have helped in more biomass accumulation in Kundan. In contrast, O_3 induced breakdown of starch and increased amounts of sucrose and enzymes associated with glycolysis have also been observed in other studies (Christ et al. 2006; Haikio et al. 2008). Under EDU treatment, carbon metabolism may have controlled stomatal movement, RuBP regeneration, and regulation of different biosynthetic pathways protecting membranes, enzymes, and other structures against O_3-induced damage, thus providing more ozone tolerance in Kundan as compared to PBW 343.

Plants response to stress conditions by triggering a network of events linked to energy metabolism. Here, we explored the role of energy metabolism–related proteins. ATP synthase subunit α (protein no.15), β (protein no. 16), ε (protein no. 17) were mostly less abundant in Kundan, whereas, in PBW, they were differentially abundant. These results showed that the energy requirement in Kundan is comparatively less under EDU protection. PBW 343 is ozone tolerant, so that it may have coped up with the normal requirement of ATP. We have also shown similar results in two wheat varieties (Gupta et al., 2018). In contrast, Sarkar et al. (2010) have shown a decreased abundance of these proteins during ozone fumigation experiments in wheat. ADP glucose pyrophosphatase (protein no. 18) was more abundant in P1. Impact on energy and electron transport chain inside the chloroplast would have improved sugar catabolism in PBW 343, proving that EDU also has effects in ozone-tolerant variety. Induction of sugar catabolism could partly be due to a need for energy and reducing power to detoxify and repair damages caused by oxidative molecules (Dizengremel 2001, Dizengremel et al. 2008; Bohler et al. 2007). Vacuolar proton ATPase (protein no. 19) was decreased in K1; depicting impact on proton pump was less as energy requirement is also less under EDU treatment in Kundan. F0-F1 ATPase (protein no. 21) was increased in P2 whereas decreased in K1 and K2. This protein

is involved in the synthesis of ATP during the light reaction by transferring electrons to the stroma. These results also proved less requirement of energy in Kundan under EDU treatment. Chloroplast proteins related to energy metabolism revealed the underlying molecular mechanism of EDU-induced protection by providing an optimum supply of energy in Kundan than PBW 343.

Rubisco LSU-binding protein (protein no. 22) was decreased in K2, whereas it increased in P1 under EDU treatment. An increase in Rubisco LSU-binding protein (chloroplastic) under EDU treatment in PBW 343 suggests that this protein may assist in the correct folding of proteins during O_3 stress. In contrast, ozone affected protein folding-related proteins in soybean (Ahsan et al. 2010). Trigger factor (protein no. 24) was differentially expressed in Kundan with increases in K2 and P2. This result showed that the trigger factor requires a higher dose of EDU for its activity. Elongation factor (protein no. 29) was less abundant in both varieties, and the Eukaryotic initiation factor (protein no. 30) was less abundant in K1, whereas more abundant in P1 and P2. These two proteins (29 and 30) participate in protein synthesis, and their less abundance in Kundan showed less EDU effects. 30S Ribosomal protein (protein no. 25) is involved in the regulation and termination of transcription (Peltier et al. 2000; Friso et al. 2004). This protein was more abundant in EDU treatment in both the varieties. This result showed EDU also affecting the transcription and regulation of protein synthesis under prevailing ozone stress in both varieties. Seventy kilodalton heat shock protein (HSP) (protein no. 28) was decreased in K1 and K2 whereas it increased in P2. It shows that EDU partially protected HSPs in Kundan during high ambient ozone. Differential abundance of TF, HSP proteins in response to O_3 stress has also been observed in other proteomic studies (Bohler et al. 2007; Cho et al. 2008; Feng et al. 2008). Twenty kilodalton chaperonin (protein no. 26) was more abundant only in K1 and P1. It assists protein folding inside the cell, thereby protecting to proteins under ozone stress. Our results showed that chaperonin requires less EDU dose for its optimal performance. Peptidyl-prolyl cis-trans isomerase (protein no. 31) was more abundant in K1 and K2 but decreased in P1 and P2. ATP-dependent Clp proteases (protein no. 27) was decreased in K2 and P2, and ATP-dependent Zinc metalloproteases (protein no. 32) were increased in Kundan whereas decreased in PBW 343 with both the EDU doses. These three proteins (31, 27, and 32) are major protein synthesis–related proteins and participate in the membrane catabolic process. Their differential responses in Kundan showed more EDU protection and less membrane disintegration as these proteins were required during membrane building. EDU protection of proteins related to synthesis and folding may have contributed towards photosynthetic and stomatal adjustment and prevention of proteins from membrane degradation under EDU treatment.

Thioredoxin H-type (TRX) (protein no. 33) had decreased abundance in Kundan, whereas it had differential abundance in PBW 343. It has a role in molecular signaling in the plant, but we found that EDU did not positively affect this protein in Kundan. Ser/Thr kinase homologous to TRX is localized at the plasma membrane and function as receptors or co-receptors in the transduction of various plant environmental and developmental signals (Dievart and Clark 2004). This means that in PBW 343, EDU may have mediated some signal to chloroplast through TRX at 200 ppm EDU treatment. Glutamine synthase (protein no. 35) was identified in both the varieties and is involved in amino acid metabolism. It was more abundant in K1 whereas less abundant in K2 and P1 under high ambient ozone. This protein performed better at 200 ppm EDU treatment in Kundan and enhanced glutamine synthesis during high ozone stress. Glycine dehydrogenase (protein no. 36) was only identified in PBW 343 and had more abundance under 300 ppm EDU. This protein catalyzes the glycine during cytosolic metabolism.

Peroxiredoxin (protein no. 37) was less abundant in P1 and contributed to maintaining defense by removing ROS inside the chloroplast. EDU treatment had no impact on this protein in Kundan. Germin-like protein (protein no. 38) was decreased in K1 and P1 whereas increased in K2. Germin-like protein (protein 38) stores nutrients required for plant metabolism, which would have helped wheat plants during ozone stress. APX (protein no. 39) was decreased at P2 and had a role in defense. However, less induction in defense-related protein may not have provided enough EDU protection against high O_3 stress. A wide range of defense-related proteins is required for biochemical adjustments and metabolic shifts, ultimately leading to the overall plant response (Castagna and Ranieri 2009). Nucleoside diphosphate kinase (NDPK) (protein no. 42) was increased in both varieties and treatments. It has a role in the transfer of phosphate group from ATP to any other nucleotide. Generally, it maintains GTP homeostasis inside the cell by transferring the phosphate group. It means EDU facilitated GTP homeostasis inside plant cells in both varieties. EDU provided optimum antioxidant defense by decreasing oxidative damage.

Pathway analysis in EDU-responsive chloroplast proteins

Proteins related to light reaction and Calvin cycle have been schematically shown in Fig. 7. In the chloroplast proteome, EDU had maximum effects on the light-harvesting complex (LHC) in Kundan. OEE (protein no. 2) was more abundant with EDU treatment in both the varieties. It has a crucial role in splitting water during non-cyclic photophosphorylation (Sugihara et al. 2000). Its increased abundance would have helped in the photolysis of water, leading to better or optimum photosynthesis. Rubisco LSU (protein no. 1) which is involved in the Calvin cycle was increased in Kundan and

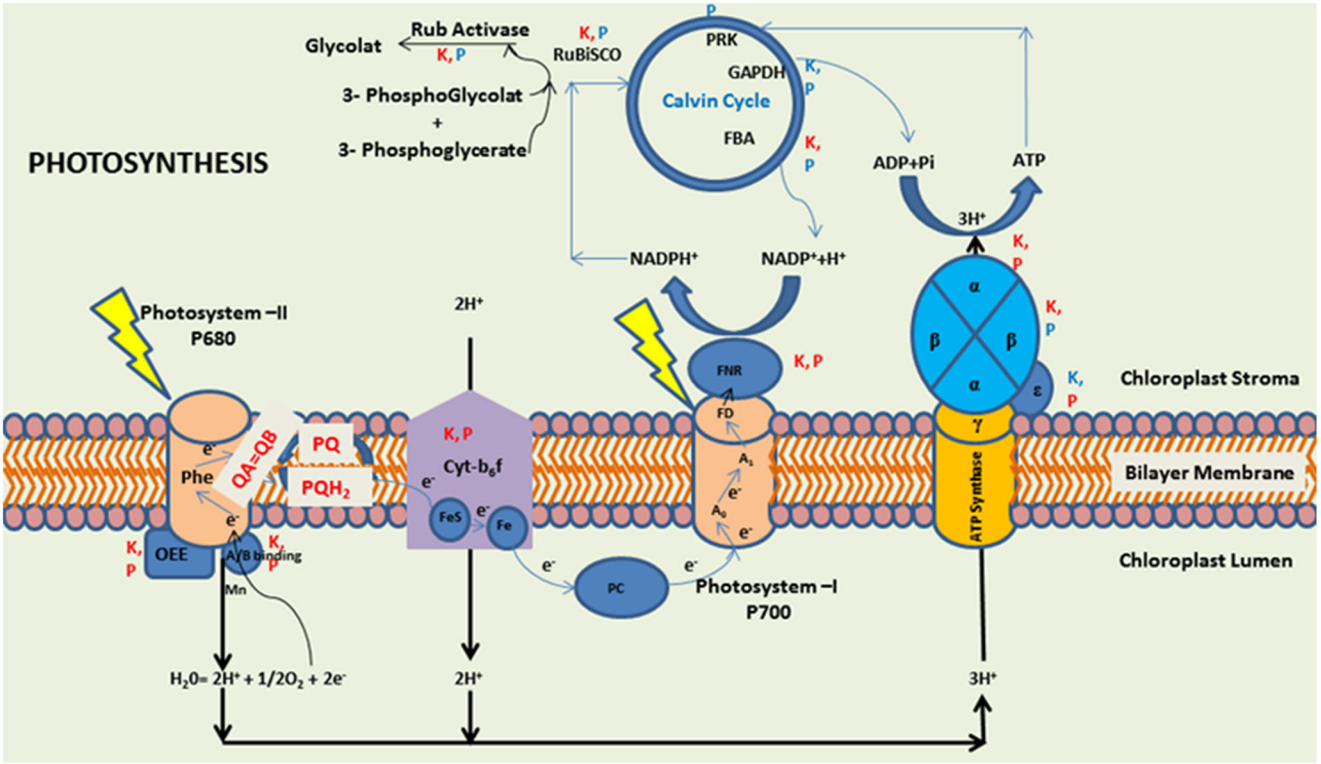

Fig. 7 Schematic representation showing effect of EDU treatment on light reaction and Calvin cycle–related chloroplastic proteins in two wheat varities: A. Kundan; B. PBW 343. Red color represents positive regulation and green represents negative regulation of proteins. (K, Kundan; P, PBW343). FBA, fructose-bisphosphate aldolase; GADPH, glyceraldehyde-3-phosphate dehydrogenase; RuBisCO, ribulose-1,5-bisphosphate carboxylase/oxygenase; PGP, Phosphoglycolat phosphtase; FNR, Ferredoxin NADP- reductase; FD, Ferredoxin; ADP, Adenosine diphosphate; ATP, Adenosine triphosphate; NADP, Nicotinamide adenine diphosphate
Abbreviations for complexes: Phe, Pheophytine; OEE, Oxygen evolving enhancer protein; Cyt b6f, Cytochrome b-6-f complex; PC, Plastocyanine

decreased in PBW 343 under EDU treatment. In contrast, the negative impact on Rubisco during ozone stress was reported in many studies (Agrawal et al. 2002; Sarkar et al. 2010). Chl a/b binding protein (protein no. 4) was increased in both the varieties, and it helps during photolysis of water. Cytb6f complex (protein no. 3) was also increased in both the EDU-treated wheat varieties. It is involved in the non-cyclic transport of electrons to plastocyanin (Kamal et al. 2013). Cho et al. (2008) reported its decreased activity in rice with ozone fumigation study. EDU protected it by minimizing ROS-generated oxidative stress. ATP synthase alpha (protein no. 15), beta (protein no. 16), and epsilon (protein no. 17) showed differential abundance during light reaction under EDU treatment. Their differential abundance revealed that EDU might have optimally protected Kundan, as the energy requirement was less, and net ATP needed for the dark reaction was also optimally provided. FNR (protein no. 5) was increased in both the varieties, whereas FBPase (protein no. 11) involved in the dark reaction was differentially abundant. FNR assists in the production of NADPH by transferring a non-cyclic electron to the ferredoxin (Kamal et al. 2013). However, FBPase was differentially abundant, so the final photosynthetic yield may not have induced under EDU treatment. Rubisco activase (protein no. 7) was increased in Kundan whereas decreased in PBW 343. It is a key enzyme to activate the Rubisco function during the dark reaction. Pathway analysis revealed that EDU has a positive impact on light reaction. However, the proteins related to dark reactions were not impacted by the EDU.

Investigating the mode of action of EDU

Based on proteomic studies of apoplast and chloroplast, a schematic representation of MAE-mediated signal transduction is presented in Fig. 6. In this figure, it has been shown how EDU induces signaling that leads to changes in cellular metabolic activities. MAE may be counteracting process as "negative effect of EDU on growth and the positive effect caused by its antioxidative properties" (Tonneijck and van Dijk 1997, 2002). A variety-specific result of EDU protection highlights the complexity of the EDU working mechanism.

We can surmise from our proteomic results that EDU first enters inside the apoplast through stomata. Paoletti et al. (2009) also reported that EDU is quickly up taken and translocated to the leaf apoplast where it persists long (>8 days), as it cannot move via the phloem. EDU is known to be rapidly transported (2 h) in the

acropetal direction, probably via the xylem stream (soil drench or stem injection application) and accumulates in the apoplastic space of the leaves (Weidensaul 1980; Roberts 1987; Gatta et al. 1997). As EDU does not enter inside cells, it indirectly affects cell metabolism. After entering the apoplast, we assume it activates one or more signaling molecule(s) (unknown) which may activate or induce ascorbate peroxidase and SOD activity inside the apoplast; we found increased activity of this protein in apoplast isolates. EDU might induce some signal that leads to activation of MAPK cascades or receptor-like kinases (RLK) in the cell. Activation of these cascades results in the better regulation of defense mechanism under high ambient ozone. This shows that perhaps EDU acts beneficially to plants via a signaling molecule (e.g., protein, protein inhibitor, or biosynthetic pathway is driven by protein activator, etc.) absent from susceptible plants (or the opposite), which remains unknown. Paoletti et al. (2008) have found increased APX and ascorbic acid and decreased apoplastic H_2O_2 and stomatal conductance in ash plants. The EDU did influence photosynthetic proteins, together with alleviating ROS-induced oxidative stress. These results concluded that EDU-induced protection against ozone phytotoxicity depends in part upon maintaining the structural integrity of cells under ozone stress, leading to enhanced cellular carbohydrate, protein, and RNA levels in leaf tissues (Lee et al. 1981; Lee and Chen 1982).

Conclusion

After analyzing the apoplast and chloroplast proteome, it can be concluded there were some unknown signaling cascades initiated after the EDU dose inside the apoplast. Apoplast proteins such as catalase, SOD, Germin-like protein, and ascorbate peroxidase helped scavenge ozone damage by maintaining optimum ROS pool under tropospheric ozone stress. Signaling cascade that started in apoplast may lead to the photosynthetic apparatus, i.e., chloroplast inside the cell and affect related regulatory proteins. In chloroplast, proteins involved in photosynthesis, energy metabolism, and PSAD had a more significant influence of EDU treatment to adopt the plant for adverse effects of ozone. For instance, some chloroplast proteins, Rubisco LSU, a/b binding protein, Rubisco activase, FNR, and proteins involved in folding/unfolding, enhanced their abundance to prove EDU protection under prevailing ozone stress. The analysis of sub-cellular organelle proteomes of wheat plants helped widen our understanding of the antioxidant defense mechanism inside and outside the apoplast and chloroplast, which related biosynthetic pathway protein abundance pattern with EDU treatment against high tropospheric ozone. This study also gives us hope for genomics, and metabolomics analysis, to increase our understanding through correlating these data together in future ozone assessment studies.

Supplementary Information The online version contains supplementary material available at https://doi.org/10.1007/s00709-021-01617-1.

Acknowledgements The authors are grateful to the Director, CSIR-NBRI, for providing the necessary facilities. SKG and MS are grateful to CSIR and UGC, respectively, for senior research fellowship.

Funding Funding for this work was provided by the Council of Scientific & Industrial Research (CSIR), New Delhi, India (project no. PSC 112).

Declarations

Conflict of interest The authors declare no competing interests.

References

Agrawal GK, Rakwal R, Yonekura M, Kubo A, Saji H (2002) Proteome analysis of differentially displayed proteins as a tool for investigating ozone stress in rice (*Oryza sativa* L.) seedlings. Proteomics 2(8): 947–959

Ahsan N, Nanjo Y, Sawada H, Kohno Y, Komatsu S (2010) Ozone stress induced proteomic changes in leaf total soluble and chloroplast proteins of soybean reveal that carbon allocation is involved in adaptation in the early developmental stage. Proteomics 10(14):2605–2619

Alves M, Francisco R, Martins I, Ricardo CPP (2006) Analysis of *Lupinus albus* leaf apoplastic proteins in response to boron deficiency. Plant Soil 279:1–11

Arnon D (1949) Estimation of Total chlorophyll. Plant Physiol 24(1):1–15

Asada K (1987) Production and scavenging of active oxygen in photosynthesis. Photoinhibition:227–287

Ashrafuzzaman M, Lubna FA, Holtkamp F, Manning WJ, Kraska T, Frei M (2017) Diagnosing ozone stress and differential tolerance in rice (*Oryza sativa* L.) with ethylenediurea (EDU). Environ Pollut 230: 339–350

Barcelo AR, Pomar F, Lopez-Serrano M, Pedreno MA (2003) Peroxidase: a multifunctional enzyme in grapevines. Funct Plant Biol 30:577–591

Betzelberger AM, Yendrek CR, Sun J, Leisner CP, Nelson RL, Ort DR, Ainsworth EA (2012) Ozone exposure response for U.S. soybean cultivars: linear reductions in photosynthetic potential, biomass, and yield. Plant Physiol 160:1827–1839

Blanco-Ward D, Ribeiro A, Paoletti E, Miranda AI (2020) Assessment of tropospheric ozone phytotoxic effects on the grapevine (*Vitis vinifera* L.): A review. Atmos Environ 117924.

Bohler S, Bagard M, Oufir M, Planchon S, Hoffmann L, Jolivet Y, Hausman JF, Dizengremel P, Renaut J (2007) A DIGE analysis of developing poplar leaves subjected to ozone reveals major changes in carbon metabolism. Proteomics 7(10):1584–1599

Bradford MM (1976) A rapid and sensitive method for the quantitation of microgram quantities of protein utilizing the principle of protein-dye binding. Anal biochem 72(1-2):248–254

Brune A, Urbach W, Dietz KJ (1994) Compartmentation and transport of zinc in barley primary leaves as basic mechanisms involved in zinc tolerance. Plant Cell Env 17(2):153–162

Brunschon-Harti S, Fangmeier A, Jager H (1995) Effects of ethylenediurea and ozone on the antioxidative system in beans (*Phaseolus vulgaris* L.). Environ Poll 90:95–103

Carnahan JE, Jenner EL, Wat EKW (1978) Prevention of ozone injury to plants by a new protectant chemical. Phytopathology 68:1225–1229

Castagna A, Ranieri A (2009) Detoxification and repair process of ozone injury: from O_3 uptake to gene expression adjustment. Environ Poll 157:1461–1469

Cavalier-Smith T (2000) Membrane heredity and early chloroplast evolution. Trends Plant Sci 5:174–182

Chameides WL (1989) The chemistry of ozone deposition to plant leave: Role of ascorbic acid. Environ Sci Technol 23:595–600

Chen Z, Gao Z, Sun Y, Wang Y, Yao Y, Zhai H, Du Y (2020) Analyzing the grape leaf proteome and photosynthetic process provides insights into the injury mechanisms of ozone stress. Plant Growth Regul 91:143–155

Cho K, Shibato J, Agrawal GK, Jung YH, Kubo A, Jwa NS, Tamogami S, Satoh K, Kikuchi S, Higashi T, Kimura S (2008) Integrated transcriptomics, proteomics, and metabolomics analyses to survey ozone responses in the leaves of rice seedling. J Proteome Res 7(7):2980–2998

Christ MM, Ainsworth EA, Nelson R, Schurr U (2006) Anticipated yield loss in field-grown soybean under elevated ozone can be avoided at the expense of leaf growth during early reproductive growth stages in favorable environmental conditions. J Exp Bot 57:2267–2275

Covarrubias AA, Ayala JW, Reyes JL, Hernandez M, Garciarrubio A (1995) Cell-wall proteins induced by water deficit in bean (*Phaseolus vulgaris* L.) seedlings. Plant physiol 107(4):1119–1128

De Leeuw FAAM, Van Zantvoort EDG (1997) Mapping of exceedances of ozone critical levels for crops and forest trees in the Netherlands: preliminary results. Environ Poll *96*(1):89–98

Dietz KJ (1997) Functions and responses of the leaf apoplast under stress. In *Progress in Botany* Springer, Berlin, Heidelberg. pp. 221-254.

Dievart A, Clark SE (2004) LRR-containing receptors regulating plant development and defense. Development 131:251–261

Dizengremel P (2001) Effects of ozone on the carbon metabolism of forest trees. Plant Physiol Bioch 39:729–742

Dizengremel P, Thiec DL, Bagard M, Jolivet Y (2008) Ozone risk assessment for plants: central role of metabolism dependent changes in reducing power. Environ Poll 156:11–15

Dunwell JM, Khuri S, Gane PJ (2000) Microbial relatives of the seed storage proteins of higher plants: conservation of structure and diversification of function during evolution of the cupin superfamily. Microbiol Mol Biol R 64(1):153–179

Emberson LD, Pleijel H, Ainsworth EA, Berg MVD, Ren W, Osborne S, Mills G, Pandey D, Dentener F, Büker P, Ewert F, Koeble R, Dingenen RV (2018) Ozone effects on crops and consideration in crop models. Eur J Agron 100:19–34

Fecht-Christoffers MM, Braun HP, Lemaitre-Guillier C, VanDorsselaer A, Horst WJ (2003) Effect of manganese toxicity on the proteome of the leaf apoplast in cowpea. Plant physiol 133(4):1935–1946

Feng ZZ, Kobayashi K, Ainsworth EA (2008) Impact of elevated ozone concentration on growth, physiology and yield of wheat (*Triticum aestivum* L.): a meta-analysis. Glob Change Biol 14:2696–2708

Fiscus EL, Booker FL, Burkey KO (2005) Crop responses to ozone: uptake, modes of action, carbon assimilation and partitioning. Plant Cell Environ 28(8):997–1011

Friso G, Giacomelli L, Ytterberg AJ, Peltier JB, Rudella A, Sun Q, van Wijk KJ (2004) In-depth analysis of the thylakoid membrane proteome of *Arabidopsis thaliana* chloroplasts: new proteins, new functions, and a plastid proteome database. The Plant Cell 16(2):478–499

Foyer CH, Noctor G (2009) Redox regulation in photosynthetic organisms: signaling, acclimation, and practical implications. Antioxid Redox Signal 11:861–905

Fuhrer J, Martin MV, Mills G, Heald CL, Harmens H, Hayes F, Sharps K, Bender J, Ashmore MR (2016) Current and future ozone risks to global terrestrial biodiversity and ecosystem processes. Ecol Evol 6: 8785–8799

Gatta L, Mancino L, Federico R (1997) Translocation and persistence of EDU (ethylenediurea) in plants: the relationship with its role in ozone damage. Environ Poll 96:445–448

Gill SS, Tuteja N (2010) Reactive oxygen species and antioxidant machinery in abiotic stress tolerance in crop plants. Plant Physiol Biochem 48:909–930

Goyer A, Haslekås C, Miginiac-Maslow M, Klein U, Le Marechal P, Jacquot JP, Decottignies P (2002) Isolation and characterization of a thioredoxin H-dependent peroxidase from *Chlamydomonas reinhardti* L. FEBS J 269(1):272–282

Green BR, Durnford DG (1996) The chlorophyll-carotenoid proteins of oxygenic photosynthesis. Annu Rev Plant Physiol Plant Mol Biol 47:685–714

Griffith M, Ala P, Yang DS, Hon WC, Moffatt BA (1992) Antifreeze protein produced endogenously in winter rye leaves. Plant Physiol 100(2):593–596

Gupta SK, Sharma M, Majumder B, Maurya VK, Lohani M, Deeba F, Pandey V (2018) Impact of Ethylene Diurea (EDU) on growth, yield and proteome of two winter wheat varieties grown under high ambient ozone phytotoxicity. Chemosphere 196:161–173

Gupta SK, Sharma M, Majumder B, Maurya VK, Deeba F, Zhang JL, Pandey V (2020) Effects of ethylenediurea (EDU) on regulatory proteins in two maize (*Zea mays* L.) varieties under high tropospheric ozone phytotoxicity. Plant Physiol Biochem 154:675–688

Haikio E, Freiwald V, Julkunen-Tiitto R, Beuker E (2008) Differences in leaf characteristics between ozone-sensitive and ozone tolerant hybrid aspen (*Populus tremula * Populus tremuloides*) clones. Tree Physiol 29:53–66

Heath RL (1980) Initial events in injury to plants by air pollutant. Annu Rev Plantt Physiol 31:395–4311

Heath RL (1988) Biochemical mechanisms of pollutant stress. In: Heck WW, Taylor OC, Tingey DT (eds) Assessment of Crop Loss from Air Pollutants. Elsevier, New York, pp 259–286

Kamal AHM, Cho K, Choi JS, Bae KH, Komatsu S, Uozumi N, Woo SH (2013) The wheat chloroplastic proteome. J proteomics 93:326–342

Kivimaenpaa M, Sellden G, Sutinen S (2005) Ozone-induced changes in the chloroplast structure of conifer needles, and their use in ozone diagnostics. Environ Poll 137(3):466–475

Kangasjärvi J, Jaspers P, Kollist H (2005) Signalling and cell death in ozone-exposed plants. Plant Cell Environ 28:1021–1036

Kerstiens G, Lendzian KJ (1989) Interaction between ozone and plant cuticles. I. ozone deposition and permeability. New Phytol 112:13–19

Kim EY, Choi YH, Lee JI, Kim IH, Nam TJ (2015) Antioxidant activity of oxygen evolving enhancer protein1 purified from *Capsosiphon fulvescens*. J Food Sci 80(6):H1412–H1417

Koistinen KM, Hassinen VH, Gynther PAM, Lehesranta SJ, Keinänen SI et al (2002) Birch PR-10c is induced by factors causing oxidative stress but appears not to confer tolerance to these agents. New Phytol 155:381–391

Lea-Smith DJ, Bombelli P, Vasudevan R, Howe CJ (2016) Photosynthetic, respiratory and extracellular electron transport pathways in cyanobacteria. Biochim Biophys Acta 1857(3):247–255

Lee EH, Bennett JH, Heggestad HF (1981) Retardation of senescence in red clover leaf discs by a new antiozonant, N- [2-(2-oxo-1-imidazolidinyl) ethyl]-N-phenylurea. Plant Physiol 67:347–350

Lee EH, Chen CM (1982) Studies on the mechanisms of ozone tolerance: Cytokinin-like activity of N-[2-(2-oxo-1-imidazolidinyl) ethyl]- N'-

phenylurea, a compound protecting against ozone injury. Physiolo Plantarum 56(4):486–491

Lee EH, Upadhyaya A, Agrawal M, Rowland RA (1997) Mechanisms of ethylenediurea (EDU) induced ozone protection: re-examination of free radical scavenger systems in snap bean exposed to O_3. Env Exp Bot 38:199–209

Lefohn AS, Malley CS, Smith L, Wells B, Hazucha M, Simon H, Naik V, Mills G, Schultz MG, Paoletti E, De Marco A, Xu XB, Zhang L, Wang T, Neufeld HS, Musselman RC, Tarasick D, Brauer M, Feng ZZ, Tang HY, Kobayashi K, Sicard P, Solberg S, Gerosa G (2018) Tropospheric ozone assessment report: global ozone metrics for climate change, human health, and crop/ecosystem research. Elementa-Sci Anthrop 6:39

Lehesranta SJ, Davies HV, Shepherd LVT, Nunan N, McNicol JW, Auriola S, Koistinen KM, Suomalainen S, Kokko HI, Kärenlampi SO (2005) Comparison of tuber proteomes of potato varieties, landraces, and genetically modified lines. Plant Physiol 138:1690–1699

Long SP, Naidu SL (2002) Effects of oxidants at the biochemical, cell and physiological levels, with reference to ozone. In: Bell JNB, Treshow M (Eds.), Air Pollution and Plant Life, second ed. Wiley, Wes Sussex, UK), pp. 69–88.

LRTAP (2017) Mapping critical levels for vegetation, chapter III of manual on methodologies and criteria for modelling and mapping critical loads and levels and air pollution effects, risks and trends. UNECE convention on long-range transboundary air pollution. On web at. Accessed date: www.icpmapping.org. (Accessed 28 June 2020).

Manning WJ, Paoletti E, Sandermann H Jr, Ernst D (2011) Ethylenediurea (EDU): a research tool for assessment and verification of the effects of ground level ozone on plants under natural conditions. Environ Poll 159:3283–3293

Mostek A, Börner A, Weidner S (2016) Comparative proteomic analysis of β-aminobutyric acid-mediated alleviation of salt stress in barley. Plant Physiol Bioch 99:150–161

Navari-Izzo F, Quartacci MF, Pinzino C, Vcchia FD, Sgherri CLM (1998) Thylakoid bound and stromal antioxidative enzymes in wheat treated with excess copper. Physiol Plantarum 104:630–638

Oksanen E, Pandey V, Pandey AK, Keski-Saari S, Kontunen-Soppela S, Sharma C (2013) Impacts of increasing ozone on Indian plants. Environ Pollut 177:189–200

Pandey AK, Majumder B, Keski-Saari S, Kontunen-Soppela S, Pandey V, Oksanen E (2014) Differences in responses of two mustard cultivars to ethylenediurea (EDU) at high ambient ozone concentrations in India. Agric Ecosyst Environ 196:158–166

Paoletti E, Contran N, Manning WJ, Castagna A, Ranieri A, Tagliaferro F (2008) Protection of ash (*Fraxinus excelsior*) trees from ozone injury by ethylenediurea (EDU): roles of biochemical changes and decreased stomatal conductance in enhancement of growth. Environ Poll 155(3):464–472

Paoletti E, Contran N, Manning WJ, Ferrara AM (2009) Use of antiozonant ethylenediurea (EDU) in Italy: verification of the effects of ambient ozone on crop plants and trees and investigation of EDU's mode of action. Environ Poll 157:1453–1460

Peltier JB, Friso G, Kalume DE, Roepstorff P, Nilsson F, Adamska I, van Wijka KJ (2000) Proteomics of the chloroplast: systematic identification and targeting analysis of lumenal and peripheral thylakoid proteins. Plant Cell 12(3):319–341

Pitcher LH, Brennan E, Zilinakas BA (1992) The antiozonant ethylenediurea does not act via superoxide dismutase induction in bean. Plant Physiol 99:1388–1392

Portis AR, Salvucci ME, Ogren WL (1986) Activation of ribulosebisphosphate carboxylase/oxygenase at physiological CO_2 and ribulose bisphosphate concentrations by Rubisco activase. Plant Physiol 82(4):967–971

Rai R (2020) Threat imposed by O_3-induced ROS on defense, nitrogen fixation, physiology, biomass allocation, and yield of legumes. In: Hasanuzzaman M, Araújo S, Gill S (eds) The Plant Family Fabaceae. Springer, Singapore, pp 503–517

Rinnan R, Holopainen T (2004) Ozone effects on the ultrastructure of peatland plants: Sphagnum mosses, *Vaccinium oxycoccus, Andromeda polifolia* and *Eriophorum vaginatum*. Ann Bot 94(4): 623–634

Roberts BR (1987) Photosynthetic response of yellow-poplar seedlings to the antioxidant chemical ethylenediurea. J Arboric 13:154–158

Roose JL, Wegener KM, Pakrasi HB (2007) The extrinsic proteins of photosystem II. Photosynth Res 92(3):369–387

Salvatori E, Fusaro L, Mereu S, Bernardini A, Puppi G, Manes F (2013) Different O_3 response of sensitive and resistant snap bean genotypes (*Phaseolus vulgaris* L.): the key role of growth stage, stomatal conductance, and PSI activity. Environ Exp Bot 87:79–91

Sanmartin M, Drogoudi PD, Lyons T, Pateraki I, Barnes J, Kanellis AK (2003) Over-expression of ascorbate oxidase in the apoplast of transgenic tobacco results in altered ascorbate and glutathione redox states and increased sensitivity to ozone. Planta 216(6):918–928

Sarkar A, Rakwal R, Bhushan Agrawal S, Shibato J, Ogawa Y, Yoshida Y, Kumar Agrawal G, Agrawal M (2010) Investigating the impact of elevated levels of ozone on tropical wheat using integrated phenotypical, physiological, biochemical, and proteomics approaches. J Proteome Res 9(9):4565–4584

Schraudner M, Ernst D, Langebartels C, Sandermann H (1992) Biochemical plant responses to ozone: III. Activation of the defense-related proteins β-1, 3-glucanase and chitinase in tobacco leaves. Plant Physiol 99(4):1321–1328

Segarra CI, Casalongue CA, Pinedo ML, Ronchi VP, Conde RD (2003) A germin like protein of wheat leaf apoplast inhibits serine proteases. J exp Bot 54(386):1335–1134

Singh S, Agrawal SB (2010) Impact of tropospheric ozone on wheat (*Triticum aestivum* L.) in the eastern Gangetic plains of India as assessed by ethylenediurea (EDU) application during different developmental stages. Agric Ecosyst Environ 138(3-4):214–221

Singh S, Agrawal S, Singh P, Agrawal M (2010) Screening three cultivars of *Vigna mungo* L. against ozone by application of ethylenediurea (EDU). Ecotoxicol Environ Saf 73:1765–1775

Sugihara K, Hanagata N, Dubinsky Z, Baba S, Karube I (2000) Molecular characterization of cDNA encoding oxygen evolving enhancer protein 1 increased by salt treatment in the mangrove *Bruguiera gymnorrhiza* L. Plant cell Physiol 41(11):1279–1285

The Royal Society (2008) Ground-level ozone in the 21st century: future trends, impacts and policy implications. In: Science Policy REPORT 15/08. The Royal Society, London report.

Thompson EW, Lane BG (1980) Relation of protein synthesis in imbibing wheat embryos to the cell-free translational capacities of bulk mRNA from dry and imbibing embryos. J Biol Chem 255(12): 5965–5970

Tonneijck AEG, Van Dijk CJ (1997) Effects of ambient ozone on injury and yield of *Phaseolus vulgaris* at four rural sites in the Netherlands as assessed by using ethylenediurea (EDU). New Phytol 135(1):93–100

Tonneijck AEG, Van Dijk CJ (2002) Injury and growth response of subterranean clover to ambient ozone as assessed by using ethylenediurea (EDU): three years of plant monitoring at four sites in The Netherlands. Environ Exp Bot 48(1):33–41

Torres NL, Cho K, Shibato J, Hirano M, Kubo A, Masuo Y, Iwahashi H, Jwa NS, Agrawal GK, Rakwal R (2007) Gel-based proteomics reveals potential novel protein markers of ozone stress in leaves of cultivated bean and maize species of Panama. Electrophoresis 28(23):4369–4381

Tran TA, Vassileva V, Petrov P, Popova LP (2013) Cadmium-induced structural disturbances in Pisum sativum leaves are alleviated by nitric oxide. Turk J Bot 37(4):698–707

Ueda Y, Siddique S, Frei M (2015) A novel gene, OZONE-RESPONSIVE APOPLASTIC PROTEIN1, enhances cell death in ozone stress in rice. Plant Physiol 169(1):873–889

Vainonen JP, Kangasjärvi J (2015) Plant signalling in acute ozone exposure. Plant Cell Environ 38(2):240–252

Vanacker H, Carver TLW, Foyer CH (1998) Pathogen-induced changes in the antioxidant status of the apoplast in barley leaves. Plant Physiol 117:1103–1114

Vandenabeele S, Van Der Kelen K, Dat J, Gadjev I, Boonefaes T et al (2003) A comprehensive analysis of hydrogen peroxide-induced gene expression in tobacco. Proc Natl Acad Sci USA 100:16113–16118

Walker DA (1980) Preparation of higher plant intact chloroplast. Method Enzymol 69:94–105

Wang GJ, Miao W, Wang JY, Ma DR, Li JQ, Chen WF (2013) Effects of exogenous abscisic acid on antioxidant system in weedy and cultivated rice with different chilling sensitivity under chilling stress. J Agron Crop Sci 199(3):200–208

Wang J, Zeng Q, Zhu J, Chen C, Liu G, Tang H (2014) Apoplastic antioxidant enzyme responses to chronic free-air ozone exposure in two different ozone-sensitive wheat cultivars. Plant physiol Biochem 82:183–193

Weidensaul TC (1980) N-(2(-2-ozo-l-imidazolidinyl)-ethyl)-N0-phenylurea as a protectant against ozone injury to laboratory fumigated pinto bean plants. Phytopathology 70:42–45

Weimar M, Rothe GM (1987) Preparation of extracts from mature spruce needles for enzymatic analyses. Physiol Plant 69:692–698

Whitaker BD, Lee EH, Rowland RA (1990) EDU and O_3 production: foliar glycerolipids and steryl lipids in snap bean exposed to O_3. Physiol Plantarum 80:286–293

Wilkinson S, Mills G, Illidge R, Davies WJ (2012) How is ozone pollution reducing our food supply? J Exp Bot 63:527–536

Willick IR, Takahashi D, Fowler DB, Uemura M, Tanino KK (2018) Tissue-specific changes in apoplastic proteins and cell wall structure during cold acclimation of winter wheat crowns. J Exp Bot 69(5):1221–1234

Yang L, Han H, Liu M, Zuo Z, Zhou K, Lü J, Zhu Y, Bai Y, Wang Y (2013) Overexpression of the *Arabidopsis* photorespiratory pathway gene, serine: glyoxylate aminotransferase (AtAGT1), leads to salt stress tolerance in transgenic duckweed (*Lemna minor*). Plant Cell Tissue Organ Cult 113(3):407–416

You J, Chan Z (2015) ROS regulation during abiotic stress responses in crop plants. Front Plant Sci 6:1092

Terms and Conditions

Springer Nature journal content, brought to you courtesy of Springer Nature Customer Service Center GmbH (“Springer Nature”).
Springer Nature supports a reasonable amount of sharing of research papers by authors, subscribers and authorised users (“Users”), for small-scale personal, non-commercial use provided that all copyright, trade and service marks and other proprietary notices are maintained. By accessing, sharing, receiving or otherwise using the Springer Nature journal content you agree to these terms of use (“Terms”). For these purposes, Springer Nature considers academic use (by researchers and students) to be non-commercial.
These Terms are supplementary and will apply in addition to any applicable website terms and conditions, a relevant site licence or a personal subscription. These Terms will prevail over any conflict or ambiguity with regards to the relevant terms, a site licence or a personal subscription (to the extent of the conflict or ambiguity only). For Creative Commons-licensed articles, the terms of the Creative Commons license used will apply.
We collect and use personal data to provide access to the Springer Nature journal content. We may also use these personal data internally within ResearchGate and Springer Nature and as agreed share it, in an anonymised way, for purposes of tracking, analysis and reporting. We will not otherwise disclose your personal data outside the ResearchGate or the Springer Nature group of companies unless we have your permission as detailed in the Privacy Policy.
While Users may use the Springer Nature journal content for small scale, personal non-commercial use, it is important to note that Users may not:

1. use such content for the purpose of providing other users with access on a regular or large scale basis or as a means to circumvent access control;
2. use such content where to do so would be considered a criminal or statutory offence in any jurisdiction, or gives rise to civil liability, or is otherwise unlawful;
3. falsely or misleadingly imply or suggest endorsement, approval , sponsorship, or association unless explicitly agreed to by Springer Nature in writing;
4. use bots or other automated methods to access the content or redirect messages
5. override any security feature or exclusionary protocol; or
6. share the content in order to create substitute for Springer Nature products or services or a systematic database of Springer Nature journal content.

In line with the restriction against commercial use, Springer Nature does not permit the creation of a product or service that creates revenue, royalties, rent or income from our content or its inclusion as part of a paid for service or for other commercial gain. Springer Nature journal content cannot be used for inter-library loans and librarians may not upload Springer Nature journal content on a large scale into their, or any other, institutional repository.
These terms of use are reviewed regularly and may be amended at any time. Springer Nature is not obligated to publish any information or content on this website and may remove it or features or functionality at our sole discretion, at any time with or without notice. Springer Nature may revoke this licence to you at any time and remove access to any copies of the Springer Nature journal content which have been saved.
To the fullest extent permitted by law, Springer Nature makes no warranties, representations or guarantees to Users, either express or implied with respect to the Springer nature journal content and all parties disclaim and waive any implied warranties or warranties imposed by law, including merchantability or fitness for any particular purpose.
Please note that these rights do not automatically extend to content, data or other material published by Springer Nature that may be licensed from third parties.
If you would like to use or distribute our Springer Nature journal content to a wider audience or on a regular basis or in any other manner not expressly permitted by these Terms, please contact Springer Nature at

onlineservice@springernature.com